Interactive comment on "Microphysical processing of aerosol particles in orographic clouds" by S. Pousse-Nottelmann et al.

Anonymous Referee #1
Received and published: 23 February 2015

We thank the referee for his/her valuable comments and suggestions. The responses (blue) to the comments (black) are below each comment.

This manuscript studied how clouds regulate aerosol and how such cloud-processed aerosol impact the subsequent cloud formation using the COSMO model coupled with the M7 aerosol module and an enhanced version of Seifert and Beheng microphysics scheme. By simulating orographic clouds over two bell-shaped mountains in an idealized two-dimensional setup, the authors identified different routes of aerosol cycles in warm- and mixed-phase clouds. It is also found that the aerosol spatial distribution, mixing state and size distribution are modified by cloud processing and such processed aerosols impact the cloud formation in downwind areas. The manuscript is well written and organized. The numerical tool and model setup are appropriate for the problem. The findings of aerosol-cloud interactions in mixed-phase clouds are important and novel. I recommend accepting this manuscript for publication after my two concerns are addressed.

1. The aerosol is still treated in a bulk manner even the size distributions and mixing states are parameterized in the model. When the regenerated aerosols are released, the proportions of different components are assigned to the same values as the background aerosols, since only one set of "dry" aerosol category is used in the model.
   The present study employs a modal approach to represent the aerosol population. Upon evaporation/sublimation, regenerated aerosol mass and number are added to the background aerosol modes potentially changing the composition and size distributions of the background aerosols and the proportion between in internally mixed/soluble and insoluble background aerosols, even if the aerosol in each grid box is assigned to only one category.

   That says, the mass of soluble and insoluble aerosols are not exactly conserved (to more precisely calculate the soluble and insoluble mass of processed aerosols, more separate sets of "regenerated aerosol" should be used).
   The aerosol module distinguishes between internally mixed/soluble and insoluble aerosol particles. Insoluble particles consist of freshly formed black/organic carbon and dust without coating. Atmospheric aging like coating with sulfate is simulated as a transfer of insoluble particles into a internally mixed/soluble mode. We apply a similar approach for processed aerosol particles. Following the homogeneous mixing assumption, we consider residual aerosol particles of evaporation and sublimation to contain an internal mixture of all foreign material in the hydrometeor. Due to sulfate production in the aqueous phase, processed particles contain some sulfate mass and therefore are attributed to the unactivated internally mixed/soluble modes. This means also that initially insoluble aerosol particles will become internally mixed/soluble after aerosol processing in clouds. The information about their initial mixing state is indeed lost once incorporated into hydrometeors. The suggested alternative approach of separate sets of "regenerated aerosol particles" would allow to analyze the compositions and size distributions of regenerated aerosol particles in more detail. However, the employed aerosol module M7 in its current state does not account for additional aerosol modes. To

allow for coagulation, sedimentation, activation and scavenging of the processed aerosol particles altogether with the unactivated background aerosol, we summed up processed and background aerosol though loosing valuable information about their specific size distributions and compositions. We now explain that more clearly.

Therefore, the difference in Aiken mode between SCAV-ALL and AP experiments showed up in Figs, 9, 10, 15 and 16. Physically, the only difference between SCAV-ALL and AP should be the enhanced accumulation and coarse modes by regenerated aerosols. However, the Aiken mode in AP is completely missed. The authors can force the Aiken mode of AP to be the same as SCAV-ALL in an ad hoc manner. And discussions on the potential impact of such deficiency should be provided in the manuscript.
In simulation AP most of the regenerated aerosol particles are released towards the Aitken and accumulation mode. We apologize for not clearly communicating these results. Regenerated Aitken mode particles have an increased size and mass compared to the background Aitken mode particles. The average radius of the "summed up" Aitken mode is increased shifting the lognormal size distribution towards larger sizes. The Aitken mode therefore appears as a hump on the lefthand side of the accumulation mode size distribution. These findings will be described more thoroughly.

2. I found the double mountain setup and general approach of this study are similar to Xue et al., 2010 and 2012. I expect to see more comparisons and discussions of the approach and results between the current one and those two studies. For example, how the cloud-processed aerosols change the riming process in downwind orographic cloud.
The setup and approach of this study are similar to the studies of Xue et al., 2010 and 2012. All three studies are based on the model intercomparison study of Muhlbauer et al., 2010. However, the treatment of aeorsol particles and the representation of aerosol processing and regeneration differs between the current and those two studies. Also, the analysis of present study focusses foremost on the impact of cloud microphysical processing on the aerosol population, whereas Xue et al., 2010 and 2012 concentrate on the implications of aerosol processing for subsequent cloud formation and properties. We agree that more comparisons and discussions between the findings of the different studies would be enriching and help to better understand the results. We will include such comparisons and discussions in the revised manuscript.

Interactive comment on "Microphysical processing of aerosol particles in orographic clouds" by S. Pousse-Nottelmann et al.

C. Knote (Referee) christoph.knote@lmu.de
Received and published: 27 February 2015

We would like to thank Christoph Knote for his elaborate and detailed suggestions and comments. There are very helpful in ameliorating the manuscript.

** Synopsis ** The authors describe a parameterization of the processing of ambient aerosol by clouds which they implemented into the mesoscale numerical weather prediction model COSMO. The authors investigate the effects of cloud passage on the development of subsequent clouds downstream by conducting 2-D idealized simulations of the flow over two hills with orographic clouds developing over both. Simulations were made with warm as well as mixed-phase clouds, and employing an existing parameterization of aerosol-cloud interactions (but without aerosol processing). The authors find strong effects on the aerosol population when including aerosol processing into their simulation, ranging from a vertical redistribution due to evaporating precipitation as well as a change in the size distribution due to cloud processing.

** General remarks **
The manuscript is well written, the methodology used is state-of-the-art and explained carefully, findings and conclusions are presented in a concise manner. The topic of the manuscript fits in the scope of Atmospheric Chemistry and Physics. A number of very interesting findings are presented and conclusions are drawn that will be useful to the aerosol community. I have a few concerns listed below which I would like to see addressed, but otherwise recommend publication in ACP.

** Major comments **

1. The authors use the modal approach to approximate the aerosol size distribution. A process acting on the size distribution can change (at most) three parameters: the overall number or mass, the median diameter and the width or shape of the distribution function (the standard deviation). It is well known that the typically observed aerosol size distribution, that is, the result of all processes acting upon the aerosol population, can be well approximated using a superposition of lognormal distribution functions. I doubt, though, that this translates directly into the validity of this approximation when describing single processes acting upon it. Let me give two simple examples:
   - activation to cloud droplets: how can one activate all particles above 35 nm (but none below) into cloud droplets, which implies removing this mass/number from the interstitial size distribution, but end up with a function that is still a lognormal? You are right that activation scavenging causes an alteration from log-normal as larger aerosol particles are removed from the modes. The scavenged aerosol mass and number are calculated as described in the model section. They correspond to the tail of the log-normal distribution. This part of the aerosol size distribution is then cut out. After activation scavenging, the remaining aerosol particles are described by new lognormal size distributions, which represents the fundamental assumption of the modal approach. Scavenging thus translates in a decrease of the peak hight of the lognormal distribution and a shift of the mode radius towards smaller sizes. In the M7 module, the standard deviations are hold fixed.
   - the efficiency of below-cloud scavenging by rain (impaction, interception) is a strong, non-linear function of the size of the particle. How does one fold a lognormal with a size-dependent function of scavenging efficiency and end up with a lognormal again?

I am well aware of the fact that this is a criticism of the modal approach in general and it is not the point made in this manuscript to address this issue. However, the processes involved in cloud processing of aerosols are prime examples of processes that, in my point of view, cannot be accurately described using a modal description of the aerosol size distribution. As investigating the effects of those processes is the aim of the authors, I am left wondering what trust we can have in the results of an investigation of these intricate details of multi-phase interactions between clouds and aerosols when the aerosol description itself is approximated in a way that is unable to reflect the processes of interest. This should at least be discussed in the methods section.

A detailed discussion of the advantages and shortcomings of the modal approach is beyond the scope of our work. Computationally cheaper, the modal approach allows to conduct 3D longterm simulations. Comparing the modal and sectional approach in a global 3D model Mann et al. (2012) found that differences between the two approaches were less than model-observation differences. However, they underline that the size-resolved aerosol properties in modal schemes need to be benchmarked and improved against sectional schemes and observations. Applying a two-moment aerosol bulk microphysics scheme with an explicit treatment of aerosol activation and scaled rates for the other microphysical processes, Lebo and Morrison (2013) obtained similar results between the modal and the sectional approach. The explicit parameterizations of aerosol activation and below-cloud scavenging processes in our model were evaluated against observations by Zubler et al. (2011). We scaled the other aerosol process rates to the cloud microphysical process rates which naturally introduces uncertainties to our results. We added this discussion.

2. The authors present a modeling study and do not compare their results against measurements. The underlying parts of the modeling system have been evaluated in a multitude of ways, but the processes added are based on a number of assumptions which bear considerable uncertainty. Hence, I deem it imperative to identify key parameters of uncertainty and conduct sensitivity studies to understand the uncertainty in the final result. As the authors already suggest in the conclusions that the next step will be realistic 3-D studies, this manuscript is somewhat of a "last chance" (and a low hanging fruit as well!) to derive uncertainties on the process level using a model setup that is simple enough so that clear connections between cause and effect can be made. Some examples: how does a wetter/dryer atmosphere affect these processes? What about very clean vs. very polluted conditions? How does overall aerosol solubility affect cloud development? As far as I understand from Zubler et al. (2011) the standard deviations of the modes are fixed, how does this affect the result? The authors stress the importance of precipitation on aerosol processing, but the warm cloud case is non-precipitating. I suggest adding a precipitating warm-cloud simulation.

We agree that the identification and evaluation of uncertainties of the final results is important. Therefore, we will broaden the present work by sensitivity studies and include the findings in the revised manuscript.

3. It is unclear from the manuscript how the transport of aerosol mass incorporated in strongly sedimenting hydrometeors (rain, graupel, ...) is treated numerically. During one time step in the model (10 s), a rain drop falling with 5-10 m/s will fall through several layers in the model. Hence at least in the operational cloud microphysics scheme in COSMO (not the 2-moment scheme used here) a special semi-implicit scheme is used to describe the sedimentation of precipitation. How is sedimentation of hydrometeors treated in the model,

and do the authors apply the same method for the in-rain / in-graupel aerosol mass (e.g. as we did in Knote and Brunner, 2013)?

The parameterization of hydrometeor sedimentation is based on corresponding number and mass weighted mean fall velocities as described in Seifert and Beheng, 2006. Within one model time step, hydrometeors may fall through several vertical model layers as the sedimentation flux calculations are done on a smaller time step. We scale the corresponding flux to the in-hydrometeor sedimentation flux.

The authors showed that there are intricate connections between the locations where the different processes take place. If the in-rain aerosol mass does not fall in the same way the rain drops do - e.g. because the in-rain sedimentation is diagnosed from the precipitation flux - the location at which it is released upon evaporation, for example, is wrong. As the authors present vertical redistribution of aerosol mass as one of the major findings, the underlying methods need to be described in more detail.

In our model, in-rain aerosol mass and rain drops fall in the same way. Therefore, the locations of rain drop evaporation and the release of a new aerosol particles upon rain drop evaporation coincide. We will describe this in more detail.

** Minor comments **

2412, 10: is the standard deviation fixed in this implementation of M7 or is it a prognostic variable?

We added:

"In M7, the aerosol number and mass concentrations are prognostic variables whereas the standard deviations are hold fixed."

2412, 11ff: the aerosol module does not include the major inorganic ions nitrate (NO3-) and ammonium (NH4+), neither does it consider thermodynamic equilibration of these semi-volatile compounds and organics (OC) with the gas-phase. NO3-, NH4+ and OC together typically constitute the majority of observed aerosol mass. The authors should at least briefly mention these omissions and discuss possible influences on the results.

We added:

"The M7 aerosol module does not account for nitrate and ammonium aerosol components as it does not include a treatment of the thermodynamic equilibration of these semi-volatile aerosol compounds with the gas phase. However, these constituents may represent an important part of the aerosol population and modify the surface properties of other aerosol particles due to coatings increasing aerosol growth and activation to cloud droplets."

2415, 4-5: this sentence reads as if the authors would know its bad but keep it for the sake of consistency. If this is the intention, it would be helpful to hint to the reader what the problem is so he/she can understand possible effects on the results. Otherwise please rephrase.

We changed it to:

"To be consistent with the standard parameterization of cloud droplet activation in the model we maintain this calculation of the updraft velocity in our simulations though not imperative at a horizontal resolution of 2 km."

2415, 11-12: see major comment - how can one cut off the tail of a lognormal and still keep a lognormal?

See answer to major comment.

2416, 26: unclear formulation: how is the scavenging by rain happening locally in a grid cell influenced by the amount of rain reaching the ground if precipitation (and hence the incorporated particles) are prognostic quantities? Please explain more thoroughly.

We changed it to:

"The parametrization is based on the scavenging coefficient following the equations in Zhao and Zheng (2006) and Croft et al. (2009), as described by Zubler et al. (2011a). In order to consider only the final removal of aerosol particles from the atmosphere by surface reaching hydrometeors, Zubler et al. (2011a) multiplied the rate change of the tracer mass and number densities due to scavenging by rain (or snow) by the fraction of precipitating rain (or snow) reaching the surface. In the new aerosol processing scheme, not only the surface reaching hydrometeors, but all precipitating rain drops and snow flakes may scavenge aerosol particles. In this scheme, the scavenging coefficients are thus independent from the fraction of surface reaching precipitation."

2416, 28ff: the reasoning that the authors omit graupel "because of the large sedimentation velocity" is not convincing as rain has even higher sedimentation velocities. Please explain and rephrase in the manuscript.
 We changed it to:
"Scavenging by falling graupel is omitted."

2420, 19-21: that is a good start - regarding the sensitivity studies mentioned in the major comments it might be interesting not only to vary the overall level of "pollution", but also consider more realistic vertical profiles (e.g. how does a dirty boundary layer influence cloud development in cleaner upper levels vs. equally dirty upper levels).
We will evaluate this suggestions for the sensitivity studies.

2424, 24-26: why do the authors need to set standard deviations, are they not given by M7?
In the setup used for this study, the standard deviation (sigma) of the Aitken and accumulation mode are adjusted to the observations. (sigma= 1.59 for the nucleation mode, sigma=2.13 for the Aitken mode, sigma=1.61 for the accumulation mode, and sigma= 2.0 for the coarse mode).

Fig 17: the isolated peak of high cloud droplet number concentrations in a) (around 750 km distance / 3500m height) seems odd - I guess this is due to the overall low liquid water content in the cold case?
You are right that the liquid water content is rather low in the cold case. The isolated peak in LWC is not taken into account in our results.

** References used **
Knote,C. and Brunner, D.: An advanced scheme for wet scavenging and liquid-phase chemistry in a regional online-coupled chemistry transport model, Atmos. Chem. Phys., 13, 1177-1192, doi:10.5194/acp-13-1177-2013, 2013.

** References used **

Mann, G. W., Carslaw, K. S., Ridley, D. A., Spracklen, D. V., Pringle, K. J., Merikanto, J., Korhonen, H., Schwarz, J. P., Lee, L. A., Manktelow, P. T., Woodhouse, M. T., Schmidt, A., Breider, T. J., Emmerson, K. M., Reddington, C. L., Chipperfield, M. P., and Pickering, S. J.: Intercomparison of modal and sectional aerosol microphysics representations within the same 3-D global chemical transport model, Atmos. Chem. Phys., 12, 4449-4476, doi:10.5194/acp-12-4449-2012, 2012.

Zachary J. Lebo and Hugh Morrison, 2013: A Novel Scheme for Parameterizing Aerosol Processing in Warm Clouds. *J. Atmos. Sci.*, **70**, 3576–3598. doi: http://dx.doi.org/10.1175/JAS-D-13-045.1

Zubler, E. M., D. Folini, U. Lohmann, D. Lüthi, A. Muhlbauer, S. Pousse-Nottelmann, C. Schär,

and M. Wild (2011), Implementation and evaluation of aerosol and cloud microphysics in a regional climate model, J. Geophys. Res., 116, D02211, doi:10.1029/2010JD014572.

Interactive comment on "Microphysical processing of aerosol particles in orographic clouds" by S. Pousse-Nottelmann et al.

Anonymous Referee #3
Received and published: 3 March 2015

We thank the referee for his/her valuable comments and suggestions.

Reply (blue) to comments (black) by referee #3 :

This paper presents parameterization of aerosol cloud processing and subsequent cloud formation in a idealized case by simulating orographic clouds over two bellshaped mountains using the numerical weather prediction model COSMO with the M7 aerosol module and an extended version of the Seifert and Beheng microphysics scheme. It is found that the aerosol-cloud processes changes aerosol composition and distribution and that cloud related aerosol cycles differs in warm phase clouds and mixed phase clouds. The processed aerosol then impacts cloud formation in downwind areas. The paper is well written and follows a organized and logical way. The used tool and setup to investigate the effects aerosol cloud processes is well chosen and is appropriate for the problem. The topic fits into Atmospheric Chemistry and Physics and the findings will be useful for further investigating aerosol cloud interactions. I recommend the publication in ACP after following concerns are addressed.

*Major issue:

There should be a major and more pronounced discussion about difference of AP and SCAV-ALL since Aitken mode is completely missed in AP in comparison to SCAV-ALL, although these to simulations expected to differ only in enhanced accumulation and coarse mode due to the regenerated aerosols.
Comparison between CTL and SCAV-ALL shows that due to scavenging processes, not only accumulation and coarse mode particles, but also an important fraction of the Aitken mode particles are removed from the interstitial aerosol particles and incorporated into cloud hydrometeors.
Further, the differences between AP and SCAV-ALL illustrate the impact of regenerated aerosol particles on the background aerosol size distributions. The differences indicate, that in AP not only accumulation and coarse mode particles, but also large Aitken mode particles are regenerated. The latter appear as a hump on the lefthand side of the accumulation mode size distribution.
These findings will be described more thoroughly.

*Minor issues:

At the time the paper of Seifert and Beheng 2006 hail was not implemented in the scheme, but newer versions does take it into account. But this has no impact on your results since you did not take hail into account.
Indeed, we did not take hail into account. We refer to the paper of Seifert and Beheng 2006 describing the version of the cloud microphysical scheme as used for the simulations.

Your Fig. 1 implies that collision scavenging is also done for graupel but text says that collision scavenging is omitted for graupel.
The figure will be corrected.

Interactive comment on "Microphysical processing of aerosol particles in orographic clouds" by S. Pousse-Nottelmann et al.

A. Bogdan
anatoli.bogdan@uibk.ac.at

Reply (blue) to comments (black) by A. Bogdan :

In the atmosphere, as in general on the Earth, water does not exist in pure state but as aqueous aerosol drops of sub/micrometer size. Cloud ice particles are formed by freezing of such drops. Since ice is highly intolerant to impurities, the freezing of sub/micrometer drops results in the formation of not pure ice but mixed-phase spherical particles: an ice core enveloped with a freeze-concentrated solution (FCS). How such coated ice cloud particles are formed and impact water vapor uptake we described in papers: Bogdan, A. and Molina, M. J. 2010,"Aqueous Aerosol May Build up an Elevated Upper Tropospheric Ice Supersaturation and Form Mixed-Phase Particles after Freezing." J. Phys. Chem. A, 114, 2821-2829; Bogdan, A. and Molina, M. J. 2009, C389 ACPD 15, C389–C390, 2015 "Why does large relative humidity with respect to ice persist in cirrus ice clouds?" J. Phys. Chem. A, 113, 14123-14130; Bogdan, A., M. J. Molina, K. Sassen, and M. Kulmala, 2006, "Formation of low-temperature cirrus from H2SO4/H2O aerosol droplets." J. Phys. Chem. A, 110, 12541-12542. Further, soon after freezing, the FCS coating around spherical ice particles will surely impact the Wegener-Bergeron-Findeisen process within mixed-phase clouds. The coated ice particles will also impact the riming process. It would be a good thing if the authors will mention the phase separation during the freezing of atmospheric aqueous drops and its impact on microphysics and development of clouds. The freeze-induced phase separation is real and the authors can find pictures and videos of this process in papers: Bogdan, A., Molina,M. J., Kulmala, M., Tenhu, H. & Loerting, T. 2013, Solution coating around ice particles of incipient cirrus clouds. Proc. Natl. Acad. Sci. USA, 11, E2439, and A. Bogdan, M. J.Molina, H. Tenhu, E. Bertel, N, Bogdan, T. Loerting, 2014, Visualization of Freezing Process in situ upon Cooling and Warming of Aqueous Solutions." Scientific reports 4: 7414 | DOI: 10.1038/srep07414.

We would like to thank Anatoli Bogdan for the valuable comments and suggestions.
We agree that a freeze-induced phase separation may have an impact on the cloud microphysics including the Wegener-Bergeron-Findeisen process and the riming process. It would be interesting to conduct a corresponding modeling study.
However, a detailed discussion of the microphysical freezing process, different freezing modes and a freeze-induced phase separation is beyond the scope of our paper.

Relevant changes made in the manuscript:

The revised manuscript comprises two new subsections regarding sensitivity test for the warm and the cold case. These sections include two new figures (Fig. 12 and 13) and two new Tables (table 5 and 6).

Microphysical processing of aerosol particles in orographic clouds

S. Pousse-Nottelmann[1,3]**, E. M. Zubler**[2]**, and U. Lohmann**[1,3]

[1]Institute for Atmospheric and Climate Science, ETH Zurich, 8092 Zurich, Switzerland
[2]Federal Office of Meteorology and Climatology MeteoSwiss, Operation Center 1, Zurich Airport, 8058 Zurich, Switzerland
[3]Center for Climate Systems Modeling, ETH Zurich, 8092 Zurich, Switzerland

Correspondence to: S. Pousse-Nottelmann (sara.pousse@env.ethz.ch)

Abstract

An explicit and detailed treatment of cloud-borne particles allowing for the consideration of aerosol cycling in clouds has been implemented in the regional weather forecast and climate model COSMO. The effects of aerosol scavenging, cloud microphysical processing and regeneration upon cloud evaporation on the aerosol population and on subsequent cloud formation are investigated. For this, two-dimensional idealized simulations of moist flow over two bell-shaped mountains were carried out varying the treatment of aerosol scavenging and regeneration processes for a warm-phase and a mixed-phase orographic cloud.

The results allowed to identify different aerosol cycling mechanisms. In the simulated non-precipitating warm-phase cloud, aerosol mass is incorporated into cloud droplets by activation scavenging and released back to the atmosphere upon cloud droplet evaporation. In the mixed-phase cloud, a first cycle comprises cloud droplet activation and evaporation via the Wegener-Bergeron-Findeisen process. A second cycle includes below-cloud scavenging by precipitating snow particles and snow sublimation and is connected to the first cycle via the riming process which transfers aerosol mass from cloud droplets to snow flakes. In the simulated mixed-phase cloud, only a negligible part of the total aerosol mass is incorporated into ice crystals. Sedimenting snow flakes reaching the surface remove aerosol mass from the atmosphere. The results show that aerosol processing and regeneration lead to a vertical redistribution of aerosol mass and number. However, the processes not only impact the total aerosol number and mass, but also the shape of the aerosol size distributions by enhancing the internally mixed/soluble Aitken and accumulation mode and generating coarse mode particles. Concerning subsequent cloud formation at the second mountain, accounting for aerosol processing and regeneration increases the cloud droplet number concentration with possible implications for the ice crystal number concentration.

1 Introduction

Orography has an important influence on precipitation formation and can be a key factor for the hydrology, ecology and climate on the local scale (Smith et al., 2005; Saleeby et al., 2009). When air is rising over sloped terrain, it cools. Above the lifting condensation level, the air be-
5 comes supersaturated with respect to water allowing for the formation of cloud droplets by condensation of water vapor onto cloud condensation nuclei (CCN). In such a warm-phase cloud, precipitation can form via condensational growth and collision-coalescence of cloud droplets. When temperatures fall below the freezing level, ice crystal formation is triggered by ice nuclei (IN), transforming the liquid cloud into a mixed-phase cloud. Due to the difference in saturation
10 vapor pressure over ice and over water, ice crystals can grow rapidly at the expense of evaporating cloud droplets when the vapor pressure is below water saturation. This process, known as the Wegener-Bergeron-Findeisen process (Wegener, 1911; Bergeron, 1935; Findeisen, 1938), can lead to a rapid glaciation of a mixed-phase cloud at temperatures between $-38\,^\circ\text{C}$ and $0\,^\circ\text{C}$. Below $-38\,^\circ\text{C}$ the droplets start to freeze homogeneously.

15 Ice microphysical processes are of major interest, as 70 % of the tropical precipitation forms via the ice phase (Lau and Wu, 2003). On the regional scale, heavy orographic precipitation events in the Alps have also been associated with ice phase processes (Pujol et al., 2005), indicating the importance of the cold phase for precipitation formation.

Aerosol particles impact the cloud microphysical processes directly by serving as cloud con-
20 densation nuclei for the formation of cloud droplets and by initiating ice nucleation. They influence cloud development and properties and ultimately precipitation formation. However, the quantification of the aerosol effect on clouds remains challenging and represents one of the largest uncertainties in the climate system (Boucher et al., 2013).

Enhanced aerosol concentrations result in an increased number concentration of cloud
25 droplets, shifting the droplet size spectrum towards smaller radii for a constant liquid water content (Twomey et al., 1974). Due to the reduced collision efficiencies of smaller droplets, the formation of rain is delayed and the cloud may persist for a longer time period (Albrecht, 1989).

3

In idealized simulations of purely warm-phase orographic precipitation, Muhlbauer and Lohmann (2008) observed that increased atmospheric aerosol concentrations lead to more but smaller cloud droplets producing a shift in precipitation towards the leeward side of the mountain (spillover effect). An investigation of orographic precipitation over the Sierra Nevada mountains showed that polluted continental aerosol concentrations in comparison to clean marine aerosol conditions lead to a precipitation reduction on the upslope side of the mountains, decreasing the overall precipitation by about 30 % (Lynn et al., 2007).

If ice processes are involved, the difference between clouds formed on marine vs. continental aerosol concentrations is even more pronounced (Lynn et al., 2007). Indeed, within mixed-phase cloud regimes, a decrease of the mean cloud droplet radius also implies a lessening of the riming efficiency between droplets and ice particles due to reduced collision efficiencies of smaller droplets (Lohmann, 2004). Saleeby et al. (2009) showed that in mixed-phase orographic clouds along the Park Range barrier in Colorado, enhanced CCN number concentrations modify the droplet distribution significantly, leading to a substantial inhibition of the riming process. At the same time, the WBF process is enhanced under polluted conditions because of the greater surface area exposure of more but smaller cloud droplets, largely compensating for the loss in snow growth by the reduced riming process (Saleeby et al., 2013).

Another important characteristic accrues from the ice-nucleation ability of certain aerosol types. Depending on the composition and mixing state, a part of the aerosol population may potentially serve as ice nuclei and trigger heterogeneous freezing. Depending on the temperature and supersaturation with respect to water, different freezing modes have been identified (Vali , 1985). Zubler et al. (2011b) showed that the effect of an increased aerosol number concentration on orographic mixed-phase clouds strongly depends on the presence of the ice phase and particularly the heterogeneous freezing of droplets. In cold simulations, with aerosol particles not only acting as CCN but also as IN in the condensation/immersion freezing mode, the reduction of precipitation formation via the liquid phase due to smaller droplets is partly compensated by a glaciation of the clouds. The processes which are most affected by increased aerosol loadings are the coalescence and riming processes (Muhlbauer and Lohmann, 2009), which are important pathways for precipitation formation.

4

Muhlbauer and Lohmann (2009) investigated the impact of dust and anthropogenic black carbon anomalies as potential ice nuclei on orographic mixed-phase clouds and pointed out the crucial role of the assumed aerosol properties. Due to the different onset temperatures and efficiencies of the different freezing modes, the ice phase may vary according to the dominant freezing process impacting the riming rate and thus the precipitation formation.

During their residence time in the atmosphere, aerosol particles undergo varying modifications which may affect their ability to serve as CCN and IN. At this, aerosol processing within clouds plays a crucial role, as the aerosol mass, composition and mixing state can be altered. Due to activation, nucleation and collision-coalescence processes aerosol particles are incorporated into hydrometeors. Processes like autoconversion, accretion, aggregation, freezing, melting, riming and selfcollection transfer aerosol mass and number between the different hydrometeor classes. Aqueous phase chemistry within droplets can lead to the formation of new aerosol mass. Finally, wet deposition, sedimentation and scavenging processes lead to a removal of aerosol mass from the atmosphere. However, a substantial fraction of hydrometeors evaporates/sublimates releasing newly formed aerosol particles to the atmosphere with different size, composition and mixing state compared to the original ones. Recent investigations concerning the impact of aerosol solubility and recycled aerosol particles on orographic cloud formation have been conducted by Xue et al. (2010, 2012). They explicitly account for the release of aerosol particles upon droplet and rain evaporation, replenishing between 1/3 to 2/3 of the scavenged aerosol particles. In their model configuration, the CCN number concentration explicitly depends on the number concentration and properties of the background and regenerated aerosol particles. In idealized 2-D simulations of warm-phase clouds over a double bell-shaped mountain, recycled aerosol particles enhance the cloud droplet number concentration and thus reduce precipitation formation at the second mountain (Xue et al., 2010). In mixed-phase clouds, regenerated aerosol particles were found to inhibit the riming process by changing the droplet size distribution (Xue et al., 2012).

In the atmosphere, however, not only cloud droplet activation, but also heterogeneous freezing processes may be affected by the release of processed aerosol particles. The ice-nucleation efficiency of aerosol particles in the different freezing modes depends on their size, composi-

tion and mixing state which may be altered during cloud processing. The present study therefore explicitly considers both, the droplet and ice nucleating ability of certain aerosol particles and their release back into the atmosphere upon evaporation/sublimation.

To better understand the role of aerosol-cloud interactions and especially the role of regen-
⁵ erated aerosol particles, the regional weather forecast and climate model COSMO has been ex-
tended by a detailed treatment of hydrometeor-borne aerosol particles following the approach by Hoose et al. (2008b). The new scheme allows for the simulation of cloud cycling of aerosols by tracing them even when scavenged into hydrometeors.

The paper is structured as follows: in Sect. 2 we describe the employed cloud and aerosol
¹⁰ microphysical parameterizations with focus on aerosol-cloud interactions. In Sect. 3 we intro-
duce the simulation setup before presenting the results for warm-phase clouds in Sect. 4.1 and mixed-phase clouds in Sect. 4.2. In Sect. 5 we end with a summary of our results and the con-
clusions.

2 Numerical model description

¹⁵ This study makes use of the non-hydrostatic, fully compressible weather prediction and climate model COSMO, which is currently developed and applied within the ~~Consortium~~ COnsortium for Small-scale ~~Modeling~~ MOdeling (COSMO, http://www.cosmo-model.org). This limited-
area mesoscale atmospheric prediction model integrates the elastic hydro-thermodynamical equations on a rotated Arakawa C-grid with a time-splitting approach following a split-explicit
²⁰ 3rd order Runge–Kutta scheme in combination with a 5th order upstream horizontal advection scheme (Doms and Schättler, 2002; Steppeler et al., 2003). The aerosol and moisture variables are advected by the second-order positive-definite Bott scheme (Bott, 1989).

2.1 Cloud microphysics

Cloud microphysical processes are calculated within the two moment bulk cloud microphysics
²⁵ scheme for water and ice clouds of Seifert and Beheng (2006). The scheme comprises prog-

6

nostic equations for the mass and number densities of five different hydrometeor classes: cloud droplets, ice crystals, rain drops, snow flakes and graupel. Warm-phase cloud processes include activation of cloud droplets, condensational growth and evaporation of cloud droplets, autoconversion (formation of rain by coagulating cloud droplets) and accretion (growth of rain drops
5 by collection of cloud droplets), selfcollection (mutual coagulation of cloud droplets/rain drops, remaining in the same drop category), evaporation of rain and collisional break-up of large rain drops. In colder regimes, the scheme also accounts for homogeneous and heterogeneous freezing, diffusional growth of ice crystals, aggregation (formation of snow by coagulating ice crystals), self-collection (mutual coagulation of ice/snow/graupel, remaining in the same hy-
10 drometeor category), riming (coagulation between the liquid and the ice phase), melting and sublimation and related secondary processes. The Wegener–Bergeron–Findeisen process is represented implicitly in the model, as in an air parcel, which is supersaturated with respect to ice, but subsaturated with respect to water, all condensate evaporates and the ice crystals grow by water diffusion. The parameterization of hydrometeor sedimentation is based on mass and
15 number weighted mean fall velocities.

2.2 Aerosol microphysics

2.2.1 The M7 aerosol module

The cloud microphysics scheme is coupled to the M7 aerosol module (Vignati et al., 2004; Muhlbauer and Lohmann, 2008, 2009; Zubler et al., 2011a) which is also used within the
20 framework of the general circulation model system ECHAM5-HAM (Stier et al., 2005). The M7 aerosol module describes the aerosol population as a superposition of seven lognormal size distributions of the form

$$N(\ln r) = \sum_{k=1}^{7} \frac{N_k}{\sqrt{2\pi} \ln \sigma_k} \exp \left[- \left(\frac{\ln r - \ln \overline{r_k}}{\sqrt{2} \ln \sigma_k} \right)^2 \right] \tag{1}$$

7

Here, N_k represents the aerosol number concentration of the kth aerosol mode with $k \in [1,7]$ and σ_k is the corresponding geometric standard deviation. In M7, the aerosol number and mass concentrations are prognostic variables whereas the standard deviations are kept constant.

The module distinguishes between four internally mixed, soluble modes (nucleation, Aitken, accumulation, and coarse mode), containing both soluble and insoluble compounds, and three insoluble modes (Aitken, accumulation, and coarse mode), which are characterized by low water solubility. It accounts for five different aerosol compounds: sulfate (SU), carbonaceous aerosols (black carbon BC, organic carbon OC), sea salt (SS) and mineral dust (DU) (Table 1). Due to sulfate coating or coagulation, insoluble particles, containing externally mixed freshly formed (black) carbon and dust, can be transferred to the internally mixed modes. The aerosol scheme accounts for nucleation of gas-phase sulfuric acid (Vehkamäki et al., 2002), condensation of sulfuric acid on pre-existing aerosol particles, coating of insoluble aerosol particles with sulfuric acid, inter- and intramodal coagulation and water vapor uptake. The M7 aerosol module does not account for nitrate and ammonium aerosol components as it does not include a treatment of the thermodynamic equilibration of these semi-volatile aerosol compounds with the gas phase. However, these constituents may represent an important part of the aerosol population and modify the surface properties of other aerosol particles due to coatings increasing aerosol growth and activation to cloud droplets. This work represents the aerosol population by the modal approach which is computationally cheaper than the sectional approach and allows to conduct 3D longterm simulations. Comparing the modal and sectional approach in a global 3D model Mann et al. (2012) found that differences between the two approaches were less than model-observation differences. However, they underline that the size-resolved aerosol properties in modal schemes need to be benchmarked and improved against sectional schemes and observations. Applying a two-moment aerosol bulk microphysics scheme with an explicit treatment of aerosol activation and scaled rates for the other microphysical processes, Lebo and Morrison (2013) obtained similar results between the modal and the sectional approach. The explicit parameterizations of aerosol activation and below-cloud scavenging processes in our model were evaluated against observations by Zubler et al. (2011a).

2.2.2 The aerosol processing scheme

To simulate aerosol processing in clouds, five new aerosol modes corresponding to the five prognostic hydrometeor classes (in-cloud droplet (CD), in-ice crystal (IC), in-rain drop (RD), in-snow flake (SF) and in-graupel (GR) aerosol mode (Table 2)) are introduced into the model.

5 Following the approach of Hoose et al. (2008b), these new modes contain hydrometeor-borne aerosol mass, potentially consisting of a contribution of all five aerosol components (SU, BC, OC, SS, DU). The number densities of hydrometeor-borne aerosol particles are no prognostic variables, but diagnosed from the corresponding hydrometeor number density during evaporation and sublimation. The new modes are not limited by any specific size range. Their median

10 radii are calculated directly upon evaporation/sublimation (Eq. 5). Aerosol activation scavenging, collision/impaction scavenging as well as sulfate production within droplets lead to an increase of the in-hydrometeor aerosol mass. In the standard version of the model as described by Muhlbauer and Lohmann (2008), the M7 aerosol module comprises the total aerosol population, including interstitial particles within the cloud, unactivated particles in cloud free air and

15 activated in-hydrometeor aerosols. In the here presented new model version, only interstitial or unactivated aerosol particles are assigned to the M7 module. All material which is taken up by a hydrometeor is transferred to the new modes CD, IC, RD, SF and GR.

Aerosol particles are incorporated into hydrometeors due to the different scavenging processes, including activation of aerosol particles, in-cloud impaction scavenging and below-cloud

20 scavenging by precipitating hydrometeors. Once inside a hydrometeor, the aerosol particles undergo the cloud microphysical processes along with the hydrometeors. Upon evaporation and sublimation, the in-hydrometeor aerosol mass is released to the atmosphere forming a newly generated aerosol particle. To allow for coagulation, sedimentation, activation and scavenging of the processed aerosol particles together with the unactivated background aerosol, processed

25 and background aerosol are summed up loosing valuable information about their specific size distributions and composition. When falling hydrometeors reach the ground, the hydrometeor-borne aerosol mass is directly removed from the system. These processes and the corresponding transfer of aerosol mass are illustrated in Fig. 1.

9

2.3 Aerosol-cloud interactions

In order to simulate aerosol-cloud interactions, the aerosol module has been coupled to the cloud microphysics scheme following the approach by Stier et al. (2005) as described in Muhlbauer and Lohmann (2008). In this standard version of the model, the aerosol number concentrations
5 influence the cloud properties, but are not affected themselves by the clouds.

The new aerosol processing scheme tracks aerosol particles even when incorporated into hydrometeors. The aerosol module M7, the cloud microphysics scheme, and the five in-hydrometeor aerosol modes are directly coupled in order to allow for the simulation of cloud cycling of aerosol particles. This enables to consider the interactions between aerosols and
10 clouds in a complete way.

2.3.1 Activation of cloud droplets

In the present model version the activation of cloud droplets is parameterized according to the approach by Lin and Leaitch (1997) following the works by Muhlbauer and Lohmann (2008) and Zubler et al. (2011a). The number of newly activated cloud droplets is based on the number
15 concentration of soluble/mixed aerosol particles larger than $35\,\mathrm{nm}$ ($N_{>35\,\mathrm{nm}}$) and the updraft vertical velocity w and is given by

$$\frac{\partial N_{\mathrm{c}}}{\partial t} = \max\left\{\frac{1}{\Delta t}\left[0.1\left(\frac{w\,N_{>35\,\mathrm{nm}}^{t}}{w + \alpha\,N_{>35\,\mathrm{nm}}^{t}}\right)^{1.27} - N_{\mathrm{c}}^{t-1}\right], 0\right\} \tag{2}$$

with $\alpha = 0.023\,\mathrm{cm^4\,s^{-1}}$ and N_{c} the number of activated cloud droplets. Especially in simulations with lower horizontal resolution the simulated vertical velocity may not reach high enough
20 values to realistically represent local updrafts when averaged over the entire gridbox. Therefore, the updraft velocity w is calculated as the sum of the grid-scale velocity w_{g} and a subgrid-scale turbulent contribution. Following the approach of Lohmann (2002) the turbulent part depends on the turbulent kinetic energy (TKE) yielding for the updraft velocity

$$w = w_{\mathrm{g}} + c_{\mathrm{turb}}\sqrt{\mathrm{TKE}}, \quad c_{\mathrm{turb}} = 1.33. \tag{3}$$

To be consistent with the standard parameterization of cloud droplet activation in the model we maintain this calculation of the updraft velocity in our simulations though not imperative at a horizontal resolution of 2 km.

$N_{>35\,\mathrm{nm}}$ is the number concentration of possible CCN particles containing all soluble/mixed aerosols in the coarse (N_4) and accumulation mode (N_3) plus the number of mixed Aitken mode particles (N_2) with a wet radius larger than $r_{\mathrm{crit}} = 35\,\mathrm{nm}$ such that

$$N_{>35\,\mathrm{nm}} = N_4 + N_3 + \int\limits_{\ln(r_{\mathrm{crit}})}^{\infty} N_2(\ln r)\mathrm{d}\ln r. \qquad (4)$$

Insoluble particles and particles smaller than 35 nm cannot act as cloud condensation nuclei. When aerosol activation scavenging is considered, the number and mass of newly activated aerosol particles are removed from the M7 aerosol module. We assume that activation scavenging is progressing from the biggest to the smallest particle in each mode. Following Zubler et al. (2011a) the scavenged mass of each species in each mode corresponds to the lognormal tail of the size distribution and is calculated using a critical radius. Scavenging thus causes a deviation from the log-normal aerosol modes, that is lost when the new log-normal size distribution with reduced number concentration and mode radius is calculated. Considering only scavenging processes without applying the aerosol processing scheme, activation scavenging implies the removal of the scavenged aerosols from the system. When the aerosol processing scheme is applied, it transfers the scavenged aerosol mass from the unactivated aerosol modes in the M7 module to the in-cloud droplet aerosol mode. In the standard version of the model, no activation scavenging is considered.

2.3.2 Heterogeneous freezing processes

Regarding heterogeneous nucleation of ice crystals, the model accounts for freezing in condensation/immersion and in contact mode (Muhlbauer and Lohmann, 2009), neglecting deposition nucleation due to the prevailing water saturation in mixed-phase clouds. The parameterization of immersion mode freezing derived from Diehl and Wurzler (2004) and Lohmann and Diehl

11

(2006) is based on the stochastic hypothesis considering that immersed aerosol particles can enhance the efficiency of random ice nucleation in a droplet, but do not disturb its stochastic nature. For immersion freezing, we consider soluble mixed black carbon (BC) and mineral dust (DU) as efficient ice nuclei dependent on a material-specific, but size-dependent freezing efficiency and on the surface area fraction (Muhlbauer and Lohmann, 2009). Heterogeneous freezing in the contact mode is parameterized following the approaches of Young (1974a), Cotton et al. (1986) and Lohmann and Diehl (2006). The freezing process is assumed to be induced by collisions between supercooled water droplets and aerosol particles by Brownian diffusion (Muhlbauer and Lohmann, 2009). We consider insoluble (hydrophobic) black carbon (BC) and mineral dust (DU) as potential nuclei for contact freezing (Diehl et al., 2006). The Brownian diffusivity decreases with increasing particle size, leading to variations of the collision efficiency of several orders of magnitude between small and larger atmospheric aerosol particles.

2.3.3 Collision scavenging

The new model version further considers scavenging of aerosol particles by collision with hydrometeors. In-cloud collision scavenging refers to collision-coalescence of aerosol particles with cloud droplets or ice crystals. The parameterization of the collision rate depends on prescribed collision kernels estimated by Young (1974b), the aerosol number concentration and the cloud droplet (ice crystal) number concentration. Collision scavenging by sedimenting rain or snow is called below-cloud scavenging. The parametrization is based on the scavenging coefficient following the equations in Zhao and Zheng (2006) and Croft et al. (2009), as described by Zubler et al. (2011a). In ~~their scheme,~~ order to consider only the final removal of aerosol particles from the atmosphere by surface reaching hydrometeors, Zubler et al. (2011a) multiplied the rate change of the tracer mass and number densities due to scavenging by rain (or snow) ~~depends also on~~ by the fraction of precipitating rain (or snow) reaching the surface. Scavenging by falling graupel is omitted~~because of the large sedimentation velocity of graupel leading to a short residence time in the atmosphere~~. In the new aerosol processing scheme, not only the surface reaching hydrometeors, but all precipitating rain drops and snow flakes may scavenge aerosol particles. In this scheme, the scavenging coefficients are thus independent

12

from the fraction of surface reaching precipitation. The scavenged aerosol mass is attributed to the corresponding in-hydrometeor aerosol mode M_{CD}^X or M_{IC}^X for in-cloud collision scavenging and M_{RD}^X or M_{SF}^X for below-cloud scavenging with $X \in \{SU, BC, OC, SS, DU\}$. The standard version of the model does not account for collision scavenging.

2.3.4 Evaporation/sublimation of hydrometeors

During evaporation and sublimation of hydrometeors, aerosol particles are released back to the atmosphere. In-hydrometeor aerosol mass and the corresponding hydrometeors are transported the same way. Within one model time step, hydrometeors may also fall through several vertical model layers as the sedimentation flux calculations are done on a smaller time step. We scale the corresponding flux to the in-hydrometeor sedimentation flux. Therefore, the locations of evaporation/sublimation and the release of a new aerosol particles upon evaporation/sublimation coincide. The emitted aerosol particles are assumed to not break up (Mitra et al., 1992) and considered to contain a mixture of all foreign material in the hydrometeor as suggested by the homogeneous mixing assumption. Due to sulfate production in the aqueous phase, all processed particles contain some sulfate mass and therefore are attributed to the unactivated internally mixed/soluble modes. Adopting lognormal size distributions for the newly formed aerosols, the dry median radius is calculated following Hoose et al. (2008b) such that

$$\overline{r}_j = \sqrt[3]{\frac{3}{4\pi} \frac{V_j^{\text{tot}}}{N_j} \frac{1}{\exp\left(1.5 \ln^2 \sigma_j\right)}}, \quad j \in \{CD, IC, RD, SF, GR\} \tag{5}$$

N_j denotes the number density of potentially released aerosol particles (equal to the number density of the corresponding hydrometeors), σ_j is the geometric standard deviation of the size distribution being fixed to the value of the corresponding unactivated aerosol mode. V_j^{tot} represents the total in-hydrometeor volume of aerosol mass within the grid box as given by

$$V_j^{\text{tot}} = \sum_l \frac{M_j^X}{\rho_X}, \quad X \in \{SU, BC, OC, SS, DU\} \tag{6}$$

13

The dry densities of the compounds are given by $\rho_{SU} = 1.841\,\mathrm{g\,cm^{-3}}$, $\rho_{BC} = \rho_{OC} = 2.0\,\mathrm{g\,cm^{-3}}$, $\rho_{SS} = 2.165\,\mathrm{g\,cm^{-3}}$ and $\rho_{DU} = 2.65\,\mathrm{g\,cm^{-3}}$ (Hoose et al., 2008b). The released aerosol particle is ~~attributed~~ added to the unactivated soluble mixed mode with $\bar{r}_m$ falling in its size range (Table 1).

3 Model setup

The present study focuses on the simulation of moist flow over a double bell-shaped mountain in order to investigate the influence of processed aerosols on orographic cloud formation. The setup is based on the works of Muhlbauer and Lohmann (2008) and Muhlbauer et al. (2010). The two-dimensional computational domain comprises 500 horizontal grid points with a grid spacing of 2 km yielding a domain size of 1000 km. In the vertical, 50 levels follow hybrid height-based Gal–Chen coordinates from the surface to the top of the computational domain at 22 km. The vertical grid spacing varies between 10 m for the lowest model level and 1000 m for the highest level. The model time step is 10 s. At the bottom of the domain we impose a free-slip boundary condition. To minimize the reflection of gravity waves from the upper model boundary, a Rayleigh Damping sponge layer fills the upper part of the computational domain beginning at an altitude of 11 km. The idealized topography consists of two identical bell-shaped mountains, each following the form given by Kirshbaum and Durran (2004):

$$h(x) = \begin{cases} \frac{h_0}{16}\left[1 + \cos\left(\pi\frac{x-x_i}{4a}\right)\right]^4, & |x-x_i| < 4a \\ 0, & |x-x_i| > 4a \end{cases} \tag{7}$$

with $h_0 = 800\,\mathrm{m}$ the mountain peak height, $a = 20\,\mathrm{km}$ the mountain half-width and x_i the horizontal position of the mountain peak with $i \in \{1,2\}$. The two mountain peaks are located at $x_1 = 600\,\mathrm{km}$ and $x_2 = 800\,\mathrm{km}$, implying a distance of 200 km between the two mountain peaks. In the present setup, aerosol particles may be processed by the cloud over the first mountain, and then advected towards the second mountain where the processed aerosol particles potentially influence further cloud formation.

14

3.1 Dynamical initialization

The temperature and humidity profiles are initialized following the work of Muhlbauer and Lohmann (2008). The initial temperature profile is calculated analytically following Clark and Farley (1984) based on the sea-level pressure p_{SL}, sea-level temperature T_{SL} and dry Brunt–
5   Väisälä frequency N_d. The sea-level pressure is fixed to $p_{SL} = 1000\,\mathrm{hPa}$ and the dry Brunt–Väisälä frequency is prescribed vertically constant with $N_d = 0.011\,\mathrm{s^{-1}}$ (Muhlbauer et al., 2010). The sea-level temperature varies between $T_{SL} = 280\,\mathrm{K}$ and $T_{SL} = 270\,\mathrm{K}$ to allow for the formation of warm-phase and mixed-phase clouds. The relative humidity profile is calculated using a modified Fermi function (Spichtinger, 2004) given by

$$
10 \quad \mathrm{RH}(z) = a + \frac{b - a}{1 + \exp(-c(z - z_0))} \tag{8}
$$

with the parameters $a = 0.90$, $b = 0.03$, $c = 0.0015\,\mathrm{m^{-1}}$ and $z_0 = 5000\,\mathrm{m}$. At the surface, the prescribed relative humidity profile has a value of $\mathrm{RH} = 0.90$ which smoothly decreases with height to a value of $\mathrm{RH} = 0.03$. The corresponding vertical profiles of temperature (blue) and dew point temperature (red) are shown in Fig. 2. Solid lines indicate the cold profiles and dashed
15   lines indicate the warm profiles. Following the setup of Muhlbauer et al. (2010) the horizontal wind speed U is vertically constant with $15\,\mathrm{ms^{-1}}$ up to an altitude of $10\,\mathrm{km}$. It then increases linearly with height up to $40\,\mathrm{ms^{-1}}$ at the top of the model domain. The initial conditions as specified yield a dimensionless mountain height $N_d h_0 / U = 0.59$. According to theoretical considerations of dry flow past topography (e.g. Durran, 1990), one thus expects an unblocked regime
20   with flow over the ridge and associated formation of gravity waves. In our simulations, however, the dynamics of the flow will be modified by latent heat release resulting from condensation. As we focus on microphysical effects only, the complexity of this aerosol-cloud interaction study is reduced by turning off the radiation scheme and the convection parameterization.

3.2 Aerosol initialization

The initial aerosol number concentrations are prescribed based on observations in order to simulate realistic atmospheric aerosol conditions (Fig. 3). The aerosol number concentrations are compiled from measurement data collected by a scanning mobility particle sizer (SMPS) during a field campaign in 1999 at the high Alpine research station Jungfrauchjoch (Weingartner et al., 1999). Throughout this study we use the average summer time aerosol size distribution as described by Muhlbauer and Lohmann (2008), which is representative for planetary boundary layer air in the Alpine region. During the summer months, convective processes and local circulations allow for the transport of boundary layer air including local anthropogenic emissions to the free troposphere (Weingartner et al., 1999). The initial aerosol composition is based on observations of aerosol mass spectrometry at the same location (see Fig. 11 in Cozic et al., 2008). Aerosol particles are internal mixtures of black carbon (BC), organic carbon (OC), sulfate (SU) and dust (DU). The first three compounds are, besides nitrates, frequently observed in central Switzerland (Hueglin et al., 2005). Dust can be occasionally observed at the Jungfraujoch during intense Saharan dust events (Cozic et al., 2008; Chou et al., 2011). The aerosol number and mass concentrations are prescribed constant with height based on the parameters for the aerosol size distributions given in Table 3.

Sulfate nucleation mode particles are formed by gas-to-particle conversion from gas-phase sulfuric acid at low temperatures. Due to their small size, these particles cannot be measured by the SMPS. The vertical profiles of gaseous sulfate and the nucleation mode aerosol particles are therefore initialized with averaged pseudosoundings taken from the global circulation model ECHAM5-HAM (Stier et al., 2005) for the nearest Jungfraujoch grid point as described by Muhlbauer and Lohmann (2008).

To investigate the impact of aerosol processing and regeneration on the aerosol size distribution and further cloud formation, we vary the complexity of the representation of aerosol processes within the model. The control simulation (CTL-w and CTL-c respectively) employs the standard version of the aerosol module M7 without any scavenging processes (Muhlbauer and Lohmann, 2008, 2009) for the warm (w) and cold (c) case. The simulations SCAV-w and SCAV-

c include aerosol activation scavenging and below-cloud scavenging as described by Zubler et al. (2011a). In the simulations AP-w and AP-c we explicitly account for the new aerosol processing scheme including detailed aerosol activation, in-cloud and below-cloud scavenging processes, aerosol processing in clouds and aerosol regeneration upon hydrometeor evaporation and sublimation as described in the model section of this paper (Table 4). To isolate the effect of aerosol regeneration, we additionally conduct simulations with the same parameterizations of the scavenging processes as in simulation AP-w and AP-c, but without aerosol regeneration (SCAV-ALL-w and SCAV-ALL-c).

4 Results

The following analyses are conducted after 10 h of simulation time, when a steady flow has been established and processed air masses from the first mountain pass over the second mountain. After 10 h, a hydrostatic mountain wave has developed with upstream regions of flow deceleration and downstream regions of flow acceleration. The upstream region is characterized by almost horizontal isentropes while the gravity wave generates foehn-like winds on the leeward side of the ridge.

4.1 Warm-phase cloud

This section focuses on the simulations initialized with the warm temperature profile with a surface temperature of 280 K. Similar dynamical conditions in all four simulations lead to the formation of warm-phase orographic clouds on the upslope side of the mountains with comparable liquid water mixing ratios (not shown). In the control simulation CTL-w, the cloud water mixing ratio has a maximum value of $0.97\,\mathrm{g\,kg^{-1}}$ over the mountain ridge (Fig. 4), whereas the rain water mixing ratio does not exceed $0.01\,\mathrm{g\,kg^{-1}}$ (not shown). In the other simulations ~~similar~~ comparable values are produced at the first mountain. In a similar setup, Xue et al. (2010) obtained a maximum cloud water mixing ratio of more than $0.7\,\mathrm{g\,kg^{-1}}$ and a maximum rain water mixing ratio between $0.01\,\mathrm{g\,kg^{-1}}$ for a dry and $0.12\,\mathrm{g\,kg^{-1}}$ for a wet environment.

17

The generated clouds are almost entirely composed of cloud droplets, producing only a negligible amount of rain. Newly formed rain drops are subsequently evaporated within the same time step as no significant amount of precipitation remains in the atmosphere or falls to the surface. The four simulations differ regarding the treatment of aerosol scavenging and regeneration processes which directly impacts the aerosol population. This becomes apparent in the number concentration of internally mixed/soluble aerosol particles larger than $35\,\mathrm{nm}$ $N_{>35\,\mathrm{nm}}$ (Fig. 5), which represents the number concentration of potential CCN in the model. In simulation CTL-w, where aerosol scavenging and regeneration processes are neglected, the aerosol number concentration $N_{>35\,\mathrm{nm}}$ is only affected by the dynamical flow over the mountain leading to a minor variation between 325 and 400 particles per cm^3. The impact of activation and below-cloud scavenging becomes apparent in simulation SCAV-w where $N_{>35\,\mathrm{nm}}$ is significantly reduced down to 200 particles per cm^3 in air masses which have passed through a cloud. Cloud droplet formation and collisions between aerosol particles and sedimenting hydrometeors reaching the surface efficiently scavenge aerosol particles in the region above the mountains. The corresponding air masses are then advected downstream so that reduced aerosol concentrations can be observed in the entire lower part of the model domain downstream of the first mountain. Simulation SCAV-ALL-w includes in-cloud collision scavenging and a more explicit treatment of below-cloud scavenging, as collisions with all sedimenting hydrometeors and not only with the ones reaching the surface are considered. In this simulation, $N_{>35\,\mathrm{nm}}$ shows a similar pattern. In-cloud collisions mainly involve Aitken mode particles, which only represent a small subset of $N_{>35\,\mathrm{nm}}$. In simulation AP-w some of the scavenged aerosol particles are replenished by aerosol regeneration upon evaporation in the downdraft region at the downslope side of the mountains. Since the prevailing wind in the simulations is unidirectional, most of the regenerated aerosol particles released upon evaporation in the first cloud are directly advected downstream towards the second mountain where they may impact further cloud formation.

However, before being released upon evaporation, in-hydrometeor aerosol particles are subject to aerosol processing within the cloud. The transfer rates for in-hydrometeor aerosol mass illustrate the importance of the different microphysical processes for cloud processing of aerosol mass. The aerosol mass transfer rates after $10\,\mathrm{h}$ of simulation time for the cloud over the first

18

mountain are shown in Fig. 6. Aerosol activation denotes the condensation of water vapor onto aerosol particles leading to the formation of cloud droplets. Aerosol activation and thus cloud droplet formation occurs on the upslope side of the mountain between 60 and 20 km ahead of the mountain crest (540–580 km) where the cloud starts to form. Other processes which can potentially transfer aerosol mass from the unactivated aerosol modes into the in-hydrometeor modes are in-cloud impaction scavenging and below-cloud scavenging. However, in the present cloud, their contributions to the total in-hydrometeor aerosol mass remain negligible. A large part of in-droplet aerosol mass is released back to the unactivated aerosol modes upon cloud droplet evaporation. Most of the aerosol reemission occurs behind the mountain crest between 600 and 630 km on the downslope side of the mountain. The other microphysical processes generate insignificant transfer rates.

The recycled aerosol particles are reattributed to the free aerosol modes changing the size distribution and total number concentration of the interstitial or unactivated aerosol particles. Figure 7 depicts the vertical profile of $N_{>35\,\mathrm{nm}}$ upstream (left panel) and downstream (right panel) of the first cloud. Upstream of the first mountain, the four simulations exhibit the same constant vertical profile of $N_{>35\,\mathrm{nm}}$ with an average value of 360 particles per cm^3. After passage over the first mountain, the simulations show distinctly different vertical profiles. In simulation CTL-w the almost constant vertical profile is conserved. The other simulations reveal a reduction in $N_{>35\,\mathrm{nm}}$ from the surface up to an altitude of 3700 m. Simulations SCAV-w and SCAV-ALL-w include an almost constant reduction to around 220 particles per cm^{-3} with considerable variations in the lower 1000 m. The strong peak at about 600 m altitude corresponds to new droplet formation between the two mountains. As the differences between these two simulations remain small, in-cloud scavenging and the adapted below-cloud scavenging parameterization accounting for all aerosol-hydrometeor collisions have only a negligible impact on $N_{>35\,\mathrm{nm}}$ in the present setup. In simulation AP-w, the loss in $N_{>35\,\mathrm{nm}}$ is partly replenished maintaining a similar pattern in the vertical profile as in simulations SCAV-w and SCAV-ALL-w.

The total aerosol mass density also shows varying vertical profiles for the different simulations downstream of the first mountain (Fig. 8 right panel). In simulation CTL-w the verti-

cal profile is conserved upstream and downstream of the mountain. Simulations SCAV-w and SCAV-ALL-w reveal similar vertical profiles with a reduction of the total aerosol mass density up to an altitude of 3700 m. The observed variations in the lower 1000 m due to new cloud formation between the mountains are also reflected in the profiles of the aerosol mass density. Simulation AP-w shows that most of the scavenged aerosol mass is replenished by evaporation throughout the column. In the lowest 1000 m the vertical profile follows the same pattern as in simulation SCAV-w and SCAV-ALL-w.

The mean cumulative aerosol number and mass concentrations of the Aitken, accumulation and coarse mode downstream of the first orographic cloud at 300 and 2000 m altitude are depicted in Figs. 9 and 10. The size distributions are calculated from the simulated values for the number concentrations and dry radii of the different aerosol modes. To obtain representative values for the processed air masses after passage over the mountain, the variables are averaged horizontally between 680 km and 720 km. We adopt the standard deviation from the initial measurements for the nucleation ($\sigma = 2.13$) and Aitken mode ($\sigma = 1.61$) and the prescribed value in the COSMO model for the coarse mode ($\sigma = 2.0$). The number size distributions (Figs. 9a and 10a) are characterized by a bimodal shape of Aitken and accumulation mode particles. Differences between the initial aerosol number concentration and CTL-w are due to aerosol coagulation and sedimentation processes, as the corresponding air masses have been exposed to aerosol microphysical processes in the model domain for 10 h. After 10 h the bimodal shape of the aerosol number concentration becomes more pronounced and the number of aerosol particles in both modes is reduced. The aerosol mass distribution is dominated by accumulation mode particles, as Aitken mode particles are too small to contribute significantly to the total aerosol mass. A slight reduction of the aerosol mass distribution can be observed in CTL-w at 2000 m altitude (Fig. 10b). In simulation SCAV-w the scavenging processes within the orographic cloud impact the aerosol size distribution by reducing the number and mass of unactivated aerosol particles. Due to activation scavenging, $N_{>35\,nm}$ is removed from the atmosphere reducing primarily the accumulation mode number concentration and shifting the mean size of the Aitken mode towards smaller sizes. The two aerosol modes appear clearly separated and the bimodal shape of the aerosol number concentration becomes more distinct. The scavenging

20

processes also cause a decrease in the aerosol mass distribution. In simulation SCAV-ALL-w the adapted parameterizations for below-cloud scavenging and in-cloud collision scavenging between interstitial aerosol particles and cloud droplets induce an additional decrease in Aitken mode particles compared to simulation SCAV-w. A sensitivity test revealed that this reduction

5 is mainly due to in-cloud collision scavenging. No significant impact on the aerosol mass distribution can be observed, as Aitken mode particles account for only a negligible fraction of the aerosol mass due to their small size. In simulation AP-w, part of the processed aerosol particles are regenerated upon evaporation, increasing the number concentration and mass of aerosol particles compared to SCAV-ALL-w. The release of processed aerosol particles pri-

10 marily increases the number concentration of the Aitken and accumulation mode along with a gain in the aerosol mass distribution compared to SCAV-ALL-w. Regenerated Aitken mode particles have an increased size and mass compared to the background Aitken mode particles. Therefore, the average radius of the combined Aitken mode is increased shifting the lognormal size distribution towards larger sizes. The Aitken mode thus appears as a hump on the lefthand

15 side of the accumulation mode size distribution. At 2000 m altitude, the aerosol mass distribution reveals the formation of some large coarse mode particles, which impact the aerosol mass distribution, but not the aerosol number concentration.

As aerosol particles act as CCN for cloud droplet formation, the changes in the aerosol size distributions impact cloud formation at the second mountain. The cloud droplet number con-

20 centration in simulation AP-w after 10 h over the second mountain and the difference in cloud droplet number concentration between simulations AP-w and SCAV-ALL-w are depicted in Figure 11a and b. In simulation AP-w, significantly more cloud droplets are formed than in SCAV-ALL-w. As the liquid water content of the cloud is only marginally influenced by the modified aerosol concentrations, this translates in more, but smaller droplets. Changes in the

25 droplet size distribution potentially affect rain formation. However, as the present cloud is characterized as non-precipitating with no measurable rain water content, a potential reduction of rain water content and rain drop number concentration cannot be observed.

The difference in cloud droplet number concentration over the second mountain between simulations AP-w and CTL-w is shown in Fig. 11c. As already seen in the beginning, $N_{>35\,nm}$

is reduced in AP-w compared to CTL-w. This results in a strong diminution of the cloud droplet number concentration. Figure 11d illustrates the difference in cloud droplet number concentration over the second mountain between simulations AP-w and SCAV-w. The results are similar to Fig. 11b where the difference between simulations AP-w and SCAV-ALL-w is shown.

Based on similar vertical profiles of $N_{>35\,nm}$ in simulation SCAV-ALL-w and SCAV-w, comparable cloud droplet number concentrations are produced in both simulations. This result illustrates that in-cloud collision scavenging impacts the aerosol size distributions, but has only marginal influence on cloud droplet formation. Obviously, the lowest cloud droplet number concentrations are observed in SCAV-w and SCAV-ALL-w. As no aerosol regeneration is taken into account, all newly formed clouds droplets at the second mountain activated from aerosol particles that have not been activated at the first mountain. Xue et al. (2010) observed a similar relationship between aerosol regeneration and cloud droplet number concentration.

Sensitivity tests

In order to evaluate the uncertainties of the presented results sensitivity studies are carried out. A first set of simulations is initialized with winter time aerosol size distributions following Muhlbauer et al. (2010) and Xue et al. (2010, 2012) which represent a clean aerosol case. Accordingly, the number concentrations of the Aitken and accumulation mode are reduced to $310\,cm^{-3}$ and $40\,cm^{-3}$ respectively. The simulations generate precipitating warm-phase clouds with a maximum cloud liquid water mixing ratio of $0.76\,g\,kg^{-1}$ and a maximum rain water mixing ratio of $0.10\,g\,kg^{-1}$ at the first mountain. As expected, the cloud water content is reduced and the rain water content is increased in the clean simulations as compared to the more polluted warm case presented before. Aerosol mass transfer rates for the corresponding simulation with aerosol processing are depicted in Figure 12. In this simulation, the aerosol mass transfer rates by activation scavenging and aerosol regeneration upon cloud droplet evaporation prevail. Aerosol mass transfer into rain drops by collisions and autoconversion, and subsequent removal by precipitation or regeneration by evaporating rain drops play a minor role. In a cloud with enhanced rain water content, these rates might be increased. The cumulative aerosol number and mass size distributions for the different clean case simulations averaged between

22

680 km and 720 km at an altitude of 300 m are displayed in Figure 13 . Aerosol scavenging in simulation SCAV and SCAV-ALL reduces the number of aerosol particles in the Aitken and accumulation mode and foremost shifts the Aitken mode towards smaller radii. The impact of aerosol regeneration can be identified as a small increase in the number concentrations of both aerosol modes and a shift of the Aitken mode towards larger radii. These findings accord with the results of the polluted warm case.

In the employed model configuration, the standard deviations of the log-normal aerosol size distributions are based on observations ($\sigma = 1.59$ for the nucleation, $\sigma = 2.13$ for the Aitken, $\sigma = 1.61$ for the accumulation, and $\sigma = 2.0$ for the coarse mode). To investigate the dependence of the results on the standard deviation, we conducted a set of simulations employing the M7 standard deviations which are 1.59 for the nucleation, Aitken and accumulation and 2.0 for the coarse mode. The standard deviations have fixed values in the model. Further sensitivity experiments include simulations with a reduced surface relative humidity of 85% and 80%.

In order to evaluate the impact of aerosol processing and regeneration on the aerosol population and on the number concentration of possible CCN in the model, the aerosol population in a sample domain downstream of the first mountain between 680 km and 720 km is analyzed. The results at 300 m and 2000 m altitude are summarized in Table 5. N_{reg} denotes the difference in the total aerosol particles number concentration averaged over the sample area between simulations AP and SCAV-ALL and thus represents the additional particles due to aerosol processing and regeneration. This number concentration is compared to the total aerosol number concentration N_{total} (Aitken, accumulation and coarse mode) in the sample area in simulation AP. A similar approach is applied for CCN by relating the difference in the CCN number concentration between simulation AP and SCAV-ALL (N_{reg}^{CCN}) to the CCN number concentration in simulation AP (N_{total}^{CCN}). In the aerosol polluted experiments, regenerated aerosol particles account for 23-39% of the total aerosol particles and for 33-47% of the CCN particles at 300 m altitude. Their contributions are slightly reduced to 18-23% to the total aerosol particles and to 32-30% to the possible CCN at 2000 m altitude. In the two clean cases, regenerated particles represent less than 10% of the total aerosol particles. However, they

account for 35-46% of the CCN particles. In the clean experiments, the aerosol population is mainly composed of Aitken mode particles as can be seen in Figure 13.

In order to evaluate how many of the scavenged aerosol particles are recycled by the cloud, the difference of the aerosol concentrations between simulation SCAV-ALL and CTL (N_{scav}) is calculated. N_{scav} represents the missing particles due to scavenging processes. The relation between N_{reg} and N_{scav} thus shows how many of the missing particles due to scavenging are replenished by regenerated particles. In the polluted experiments, this relation ranges between 24 and 39% representing about 1/4 to 1/3 of the missing aerosol particles due to scavenging. In the clean experiments, it does not exceed 27%. These findings are lower than in the study of Xue et al. (2010) who found that regenerated particles replenish 1/3 to 2/3 of the missing particles.

The presented sensitivity experiments show that impact of regenerated aerosol particles on the aerosol and CCN number concentrations not only depends on the cloud regime but also on the aerosol population. Variations in the relative humidity or the standard deviation reveal to have a smaller influence.

4.2 Mixed-phase cloud

We employ the cold temperature profile with a surface temperature of $270\,\mathrm{K}$ to generate mixed-phase orographic clouds over the two mountains. The ascent over the bell-shaped mountains results in the formation of liquid cloud droplets on the upslope side of the mountain. After $10\,\mathrm{h}$, liquid droplets only persist at cloud base (Fig. 14). Advected aloft, they may undergo heterogeneous freezing processes to form ice crystals which constitute the upper part of the cloud. Due to the difference in saturation vapor pressure over ice and over liquid, cloud droplets may also evaporate in the presence of ice crystals allowing for the enhanced condensation of water vapor on preexisting ice crystals (Wegener-Bergeron-Findeisen process). The cloud over the first mountain consists mainly of cloud ice and snow with little cloud liquid water. In this first cloud, collision processes between ice crystals lead to the aggregation of snow flakes which sediment to the surface. A large part of the cloud water is removed from the atmosphere by sedimenting snow reducing the available water vapor in the atmosphere. Therefore, the envi-

ronment downstream of the first cloud is drier than ahead of the first cloud. The cloud over the second mountain developing in this drier environment has much less cloud ice and the snow formation processes are suppressed.

In mixed-phase clouds, a multitude of microphysical processes can take place which affect the aerosol population. In the present setup, the in-hydrometeor aerosol mass is concentrated in cloud droplets and snow, whereas the aerosol mass within ice crystals appears to be negligible. Figure 15 illustrates which processes are important in terms of the transfer of aerosol mass in and out and between the different hydrometeors. Aerosol mass is transferred into cloud droplets mostly by activation scavenging. When the cloud droplets reach higher altitudes some ice is formed heterogeneously via condensation/immersion freezing or contact freezing. Although these processes are essential for the formation of ice crystals in the model, their influence on the aerosol transfer remains negligible. In the presence of ice crystals, the liquid droplets rapidly evaporate and the water vapor condenses on the ice phase (Wegener–Bergeron–Findeisen process) when the vapor pressure is below water saturation. Therefore, cloud droplet activation and evaporation take place at the same horizontal location but in different altitudes. These two processes form a first aerosol processing cycle which acts via the liquid phase. The ice crystals grow and aggregate to form snow flakes which efficiently take up aerosol mass by riming with cloud droplets and below-cloud scavenging of interstitial aerosol particles. Sedimenting snow flakes remove aerosol mass from the atmosphere. Downstream of the cloud, some snow flakes sublimate releasing aerosol mass back to the interstitial mode (peak at 630 km). The second aerosol processing cycle therefore covers the interactions with snow flakes. A connection between the two cycles represents the riming process which transfers aerosol mass from cloud droplets to snow flakes. The other microphysical processes within the model are negligible for the transfer of aerosol mass in the present case study.

The described processes within the first cloud have an important influence on the vertical distribution of aerosol particles. Figure 16 shows the vertical profile of the total aerosol mass for the different simulations upstream (left panel) and downstream (right panel) of the first cloud. All simulations show the same vertical profile upstream of the first mountain. In simulation CTL-c, the vertical profile remains constant after passage over the mountain. Simulation SCAV-c in-

cludes a reduction of aerosol mass in the lower 3700 m where the cloud forms. This reduction is due to activation and below-cloud scavenging. The modified scavenging parameterizations in simulation SCAV-ALL-c generate a significantly larger diminution of the aerosol mass concentration in the lower part of the atmosphere. In simulation SCAV-ALL-c, below-cloud scav-

5 enging is treated differently, as all aerosol particles colliding with sedimenting rain or snow are removed from the unactivated aerosol modes, whereas in simulation SCAV-c only the fraction corresponding to the fraction of precipitation reaching the surface is removed. Therefore, below-cloud scavenging is far more efficient in simulation SCAV-ALL-c, as apparent in the amplified reduction of the vertical profile below 2000 m altitude. Additionally, SCAV-ALL-c accounts for

10 in-cloud collision scavenging and scavenging of aerosol particles acting as contact IN. In simulation AP-c evaporation processes lead to the release of additional aerosol particles, increasing the aerosol mass compared to SCAV-ALL-c. Above about 2200 m almost all scavenged aerosol mass is replenished by aerosol regeneration upon evaporation.

The cumulative aerosol number and mass size distributions of the Aitken, accumulation and

15 coarse mode downstream of the first mountain at 300 m and 2000 m altitude are depicted in Figs. 17 and 18. The values are averaged horizontally between 680 km and 720 km. Aerosol microphysical processes like coagulation and sedimentation lead to a reduction in the aerosol number and mass size distribution after 10 h in simulation CTL-c compared to the initial aerosol size distributions. At both altitudes the bimodal shape of the aerosol number size distribution

20 becomes more distinct while both Aitken and accumulation mode are reduced. The aerosol mass size distribution determined by the accumulation mode is slightly reduced due to sedimentation. Scavenging processes in simulation SCAV-c lead to a considerable reduction in aerosol number and mass. The influence on the shape of the aerosol number size distribution becomes particularly apparent at 300 m altitude, where Aitken and accumulation mode are clearly separated by

25 a large gap. At this low altitude, the aerosol mass size distribution is significantly reduced. The reduction in aerosol mass and number at 300 m altitude is even more pronounced in simulation SCAV-ALL-c where the modified below-cloud scavenging parameterization, in-cloud collision scavenging and scavenging of contact IN remove the major part of unactivated aerosol particles from the atmosphere. A comparison with the non-precipitating warm-phase cloud suggests,

26

that an important part of the scavenging is due to the more detailed below-cloud scavenging by sedimenting snow particles. At an altitude of 2000 m below-cloud scavenging and activation scavenging become less important. The differences between AP and SCAV-ALL illustrate the impact of regenerated aerosol particles on the background aerosol size distributions. Aerosol regeneration upon droplet evaporation and snow sublimation in simulation AP-c leads to an increase in aerosol number and mass compared to simulation SCAV-ALL-c. The aerosol number size distribution reveals that foremost large Aitken and accumulation mode particles are released to the atmosphere. Newly formed Aitken mode particles have an increased size and mass as compared to the background Aitken mode particles. The log-normal distribution of the Aitken mode is shifted towards larger size and appears as a bump on the lefthand side of the accumulation mode size distribution. At 300 m altitude few coarse mode particles are formed which appear in the aerosol mass distribution.

As aerosol particles serve as CCN and/or IN, changes in the aerosol number and mass size distribution may impact the number concentration of cloud droplets and ice crystals as shown in Fig. 19. The cloud droplet number and ice crystal number concentrations over the second mountain in simulation AP-c are displayed in Fig. 19a and b, differences between simulations AP-c and SCAV-ALL-c are shown in Fig. 19c and d. The released aerosol particles in AP-c lead to an increase in cloud droplet number concentration as compared to SCAV-ALL-c. The ice crystal number concentration reveals a comparable increase as more cloud droplets and also more aerosol particles are available for heterogeneous freezing processes. However, these changes in the number concentrations do not impact the cloud liquid and ice water content noticeably.

Sensitivity tests

Several sensitivity test were carried out in order to evaluate the uncertainties of the results. We conducted simulations with a lowered surface relative humidity to 85 % and 80 %, with altered standard deviations, and with a clean (winter) aerosol initialization. The analysis focuses on the averaged aerosol population downstream of the first mountain between 680 km and 720 km. The results at an altitude of 300 m and 2000 m are summarized in Table 6. The

difference between simulations AP and SCAV-ALL (N_{reg}) is compared to the total aerosol number concentration of the Aitken, accumulation and coarse mode (N_{total}) in simulation AP. Analogously, the difference in the CCN number concentration between simulation AP and SCAV-ALL (N_{reg}^{CCN}) is related to the CCN number concentration (N_{total}^{CCN}) in simulation AP. Regenerated aerosol particles constitute between 18-28% of the total aerosol particles and between 38-57% of the CCN particles in polluted simulations. Similar as in the warm case, the clean sensitivity experiments of the cold case reveal a negligible contribution of regenerated particles to the total aerosol concentration ($< 5\%$), but constitute a considerably part of the CCN number concentration (26-55%). Further, we investigate how many of the missing particles due to scavenging are replenished by regenerated particles. N_{reg} is related to the difference of the aerosol concentrations between simulation SCAV-ALL and CTL (N_{scav}). In all sensitivity experiments at 300 m altitude, regenerated particles replenish only less than 10% of the missing particles supporting the assumption that most of the scavenged particles are removed from the atmosphere by precipitation. At 2000 m altitude, a replenishment of up to 57% can be observed.

The results show that not only the cloud but also the aerosol regime plays an important role for aerosol regeneration and its impact on the background aerosol population. For precipitating clouds, the analyzed altitude is a determining factor.

5 Summary and conclusions

The effects of warm-phase and mixed-phase orographic clouds on the aerosol population have been evaluated by simulating orographic cloud formation over a 2-D double bell-shaped topography with the regional weather forecast and climate model COSMO. An explicit treatment of in-hydrometeor aerosol mass allowing for the consideration of aerosol processing in clouds has been implemented in the model. Aerosol scavenging processes and aerosol processing in clouds including aerosol regeneration upon evaporation or sublimation affect the aerosol population greatly. At this, different aerosol cycles have been identified. In the simulated non-precipitating warm-phase cloud, aerosol mass is incorporated in cloud droplets by activation scavenging and

released back to the atmosphere upon cloud droplet evaporation. In the simulated precipitating mixed-phase cloud, a significant amount of aerosol mass can be found in cloud droplets and snow flakes, but less in ice crystals. Activation and below-cloud scavenging efficiently transfer aerosol mass in the cloud droplets and snow flakes, while ice crystals are formed heteroge-
neously from a few cloud droplets allowing only for a limited transfer of aerosol mass. In the mixed-phase clouds, two aerosol cycles were identified. A first cycle includes activation scavenging and cloud droplet evaporation due to the WBF process. A second cycle comprehends the interactions with snow flakes and is connected to the first cycle via the riming process which transfers aerosol from cloud droplets to snow flakes. As aerosol particles are transported to-
gether with the sedimenting hydrometeors a vertical redistribution of the aerosol number and mass concentration occurs with aerosol mass being transported towards lower altitudes or even being removed from the atmosphere. Precipitating snow in the lower atmosphere very efficiently removes aerosol number and mass from the atmosphere.

The present study shows that the different scavenging parameterizations and the consider-
ation of aerosol regeneration modify not only the total aerosol number and mass but also the shape of the aerosol size distributions. Accounting for aerosol processing in clouds, the scavenged aerosol particles are partly replenished by the release of aerosol particles upon hydrometeor evaporation/sublimation. The released aerosol particles mainly add to the Aitken and accumulation mode. Depending on the simulated cloud, the formation of coarse mode aerosol
particles can be observed at specific altitudes. The newly generated large coarse mode particles are possible candidates for giant cloud condensation nuclei (GCCN) which may lead to rapid rain formation in warm-phase clouds (Saleeby et al., 2009; Posselt and Lohmann, 2008). This in turn would impact the precipitation rate and the longevity of the cloud. However, the current model does not include any specific treatment of GCCN which would allow to study the impact
of these particles in more detail. The release of internally mixed aerosol particles in the accumulation and coarse modes increases the number concentration of possible CCN in the model impacting further cloud formation. The simulations show that aerosol regeneration increases the cloud droplet number concentration at the second mountain with possible implications for the ice crystal number concentration. In comparison to the standard model version, the aerosol

29

activation and below-cloud scavenging processes revealed to be most important reducing the aerosol number concentration and in turn the cloud droplet number concentration at the second mountain. An influence on the ice crystal number concentration is observable via the changes in cloud droplet number concentration. In-cloud collision scavenging mainly affects the Aitken mode without any important implications for cloud droplet formation in warm-phase clouds. Due to collision processes insoluble aerosol particles, which potentially may act as ice nuclei in the contact mode, are removed from the free atmosphere limiting the efficiency of contact freezing. Though, in the present mixed-phase clouds this effect remains negligible.

Changes in the cloud droplet and ice crystal number concentration potentially affect the formation of precipitation in the model. However, in the present setup of non-precipitating warm-phase clouds, the increase in cloud droplet number concentration does not imply any important changes for the rain formation over the second mountain. In a precipitating cloud however, the formation of more but smaller cloud droplet may impede rain formation, as autoconversion and collision efficiencies may be reduced. The influence of the variations in cloud droplet and ice crystal number concentration on the ice water content in the simulated mixed-phase clouds remains negligible. Most of the ice is formed via the Wegener-Bergeron-Findeisen process which effectively adds water vapor to the ice crystals. Due to the high efficiency of this process in the present setup the number of preexisting ice particles appears to be non-relevant for the total ice water content.

The present study focuses on the influence of aerosol processing in warm-phase and mixed-phase clouds on the aerosol population over an idealized 2-D double bell-shaped mountain. A subsequent study should investigate the implications of the modified aerosol spectrum on further cloud formation in a 3-D regional study. Special emphasis should be placed on precipitation formation and the governing cloud microphysical processes.

References

Albrecht, B. A.: Aerosols, cloud microphysics, and fractional cloudiness, Science, 245, 1227–1230, doi:10.1126/science.245.4923.1227, 1989.

Bergeron, T.: On the physics of clouds and precipitation, in: Proceedings of the 5th Assembly U.G.G.I., Lisbon, 17–24 September 1933, 2, 156–180, 1935.

Bott, A.: A positive definite advection scheme obtained by nonlinear renormalization of the advective fluxes, Mon. Weather Rev., 117, 1006–1016, doi:10.1175/1520-0493(1989)117<1006:APDASO>2.0.CO;2, 1989.

Boucher, O., Randall, D., Artaxo, P., Bretherton, C., Feingold, G., Forster, P., Kerminen, V.-M., Kondo, Y., Liao, H., Lohmann, U., Rasch, P., Satheesh, S., Sherwood, S., Stevens, B., and Zhang, X.: Clouds and aerosols, in: Climate Change 2013: The Physical Science Basis. Contribution of Working Group I to the Fifth Assessment Report of the Intergovernmental Panel on Climate Change, Cambridge University Press, Cambridge, UK and New York, NY, USA, available at: http://www.ipcc.ch/ipccreports/ar4-wg1.htm (last access: 15 July 2014), 571–657, 2013.

Chou, C., Stetzer, O., Weingartner, E., Jurányi, Z., Kanji, Z. A., and Lohmann, U.: Ice nuclei properties within a Saharan dust event at the Jungfraujoch in the Swiss Alps, Atmos. Chem. Phys., 11, 4725–4738, doi:10.5194/acp-11-4725-2011, 2011.

Clark, T. L. and Farley, R. D.: Severe downslope windstorm calculations in two and three spatial dimensions using anelastic interactive grid nesting: a possible mechanism for gustiness, J. Atmos. Sci., 41, 329–350, doi:10.1175/1520-0469(1984)041<0329:SDWCIT>2.0.CO;2, 1984.

Cotton, W. R., Tripoli, G. J., Rauber, R. M., and Mulvihill, E. A.: Numerical simulation of the effects of varying ice crystal nucleation rates and aggregation processes on orographic snowfall, J. Clim. Appl. Meteorol., 25, 1658–1680, doi:10.1175/1520-0450(1986)025<1658:NSOTEO>2.0.CO;2, 1986.

Cozic, J., Verheggen, B., Weingartner, E., Crosier, J., Bower, K. N., Flynn, M., Coe, H., Henning, S., Steinbacher, M., Henne, S., Collaud Coen, M., Petzold, A., and Baltensperger, U.: Chemical composition of free tropospheric aerosol for PM1 and coarse mode at the high alpine site Jungfraujoch, Atmos. Chem. Phys., 8, 407–423, doi:10.5194/acp-8-407-2008, 2008.

Croft, B., Lohmann, U., Martin, R. V., Stier, P., Wurzler, S., Feichter, J., Posselt, R., and Ferrachat, S.: Aerosol size-dependent below-cloud scavenging by rain and snow in the ECHAM5-HAM, Atmos. Chem. Phys., 9, 4653–4675, doi:10.5194/acp-9-4653-2009, 2009.

Diehl, K. and Wurzler, S.: Heterogeneous drop freezing in the immersion mode: model calculations considering soluble and insoluble particles in the drops, J. Atmos. Sci., 61, 2063–2072, doi:10.1175/1520-0469(2004)061<2063:HDFITI>2.0.CO;2, 2004.

Diehl, K., Simmel, M., and Wurzler, S.: Numerical sensitivity studies on the impact of aerosol properties and drop freezing modes on the glaciation, microphysics, and dynamics of clouds, J. Geophys. Res., 111, D07202, doi:10.1029/2005JD005884, 2006.

Doms, G. and Schättler, U.: A Description of the Nonhydrostatic Regional Model LM Part I: Dynamics and Numerics, Tech. rep., Deutscher Wetterdienst, Offenbach, Germany, 2002.

Durran, D. R.: Mountain waves and downslope winds, Atmospheric American Meteorological Society, Boston, 1990.

Findeisen, W.: Die kolloidmeteorologischen Vorgänge bei der Niederschlagsbildung (Colloidal meteorological processes in the formation of precipitation), Meteorol. Z., 55, 121–133, 1938.

Hoose, C., Lohmann, U., Bennartz, R., Croft, B., and Lesins, G.: Global simulations of aerosol processing in clouds, Atmos. Chem. Phys., 8, 6939–6963, doi:10.5194/acp-8-6939-2008, 2008a.

Hoose, C., Lohmann, U., Stier, P., Verheggen, B., and Weingartner, E.: Aerosol processing in mixed-phase clouds in ECHAM5-HAM: model description and comparison to observations, J. Geophys. Res., 113, D07210, doi:10.1029/2007JD009251, 2008b.

Hueglin, C., Gehrig, R., Baltensperger, U., Gysel, M., Monn, C., and Vonmont, H.: Chemical characterisation of $PM_{2.5}$, PM_{10} and coarse particles at urban, near-city and rural sites in Switzerland, Atmos. Environ., 39, 637–651, 2005.

Kirshbaum, D. J. and Durran, D. R.: Factors governing cellular convection in orographic precipitation, J. Atmos. Sci., 61, 682–698, doi:10.1175/1520-0469(2004)061<0682:FGCCIO>2.0.CO;2, 2004.

Lau, K. M. and Wu, H. T.: Warm rain processes over tropical oceans and climate implications, Geophys. Res. Lett., 30, 2290, doi:10.1029/2003GL018567, 2003.

Lebo, Zachary J. and Morrison, Hugh: A Novel Scheme for Parameterizing Aerosol Processing in Warm Clouds. J. Atmos. Sci., 70, 3576?3598, doi:10.1175/JAS-D-13-045.1, 2013.

Lin, H. and Leaitch, R.: Development of an in-cloud aerosol activation parameterization for climate modelling, Paper presented at Workshop on Measurements of Cloud Properties for Forecasts of Weather, Air Quality and Climate, World Meteorol. Soc., Mexico City, 1997.

Lohmann, U.: Can anthropogenic aerosols decrease the snowfall rate?, J. Atmos. Sci., 61, 2457–2468, doi:10.1175/1520-0469(2004)061<2457:CAADTS>2.0.CO;2, 2004.

Lohmann, U. and Diehl, K.: Sensitivity studies of the importance of dust ice nuclei for the indirect aerosol effect on stratiform mixed-phase clouds, J. Atmos. Sci., 63, 968–982, doi:10.1175/JAS3662.1, 2006.

Lohmann, U.: Possible aerosol effects on ice clouds via contact nucleation, J. Atmos. Sci., 59, 647–656, doi:10.1175/1520-0469(2001)059<0647:PAEOIC>2.0.CO;2, 2002.

Lynn, B., Khain, A., Rosenfeld, D., and Woodley, W. L.: Effects of aerosols on precipitation from orographic clouds, J. Geophys. Res., 112, D10225, doi:10.1029/2006JD007537, 2007.

Mann, G. W., Carslaw, K. S., Ridley, D. A., Spracklen, D. V., Pringle, K. J., Merikanto, J., Korhonen, H., Schwarz, J. P., Lee, L. A., Manktelow, P. T., Woodhouse, M. T., Schmidt, A., Breider, T. J., Emmerson,

K. M., Reddington, C. L., Chipperfield, M. P., and Pickering, S. J.: Intercomparison of modal and sectional aerosol microphysics representations within the same 3-D global chemical transport model, Atmos. Chem. Phys., 12, 4449-4476, doi:10.5194/acp-12-4449-2012, 2012.

Mitra, S., Brinkmann, J., and Pruppacher, H.: A wind tunnel study on the drop-to-particle conversion, J. Aerosol Sci., 23, 245–256, doi:10.1016/0021-8502(92)90326-Q, 1992.

Muhlbauer, A. and Lohmann, U.: Sensitivity studies of the role of aerosols in warm-phase orographic precipitation in different dynamical flow regimes, J. Atmos. Sci., 65, 2522–2542, doi:10.1175/2007JAS2492.1, 2008.

Muhlbauer, A. and Lohmann, U.: Sensitivity studies of aerosol-cloud interactions in mixed-phase orographic precipitation, J. Atmos. Sci., 66, 2517–2538, doi:10.1175/2009JAS3001.1, 2009.

Muhlbauer, A., Hashino, T., Xue, L., Teller, A., Lohmann, U., Rasmussen, R. M., Geresdi, I., and Pan, Z.: Intercomparison of aerosol-cloud-precipitation interactions in stratiform orographic mixed-phase clouds, Atmos. Chem. Phys., 10, 8173–8196, doi:10.5194/acp-10-8173-2010, 2010.

Posselt, R. and Lohmann, U.: Influence of Giant CCN on warm rain processes in the ECHAM5 GCM, Atmos. Chem. Phys., 8, 3769–3788, doi:10.5194/acp-8-3769-2008, 2008.

Pujol, O., Georgis, J.-F., Chong, M., and Roux, F.: Dynamics and microphysics of orographic precipitation during MAP IOP3, Q. J. Roy. Meteor. Soc., 131, 2795–2819, doi:10.1256/qj.04.79, 2005.

Saleeby, S. M., Cotton, W. R., Lowenthal, D., Borys, R. D., and Wetzel, M. A.: Influence of cloud condensation nuclei on orographic snowfall, J. Appl. Meteorol. Clim., 48, 903–922, doi:10.1175/2008JAMC1989.1, 2009.

Saleeby, S. M., Cotton, W. R., Lowenthal, D., and Messina, J.: Aerosol impacts on the microphysical growth processes of orographic snowfall, J. Appl. Meteorol. Clim., 52, 834–852, doi:10.1175/JAMC-D-12-0193.1, 2013.

Seifert, A. and Beheng, K. D.: A two-moment cloud microphysics parameterization for mixed-phase clouds. Part 1: Model description, Meteorol. Atmos. Phys., 92, 45–66, doi:10.1007/s00703-005-0112-4, 2006.

Smith, R. B., Barstad, I., and Bonneau, L.: Orographic precipitation and Oregon's climate transition, J. Atmos. Sci., 62, 177–191, doi:10.1175/JAS-3376.1, 2005.

Spichtinger, P.: Eisübersättigte Regionen, Forschungsbericht FB-2004-21, Deutsches Zentrum für Luft und Raumfahrt, Ph.D. Thesis, Oberpfaffenhofen, 211 pp., 2004.

Steppeler, J., Doms, G., Schättler, U., Bitzer, H. W., Gassmann, A., Damrath, U., and Gregoric, G.: Meso-gamma scale forecasts using the nonhydrostatic model LM, Meteorol. Atmos. Phys., 82, 75–96, doi:10.1007/s00703-001-0592-9, 2003.

Stier, P., Feichter, J., Kinne, S., Kloster, S., Vignati, E., Wilson, J., Ganzeveld, L., Tegen, I., Werner, M., Balkanski, Y., Schulz, M., Boucher, O., Minikin, A., and Petzold, A.: The aerosol–climate model ECHAM5-HAM, Atmos. Chem. Phys., 5, 1125–1156, doi:10.5194/acp-5-1125-2005, 2005.

Twomey, S. A., Piepgrass, M., and Wolfe, T. L.: An assessment of the impact of pollution on global cloud albedo, Tellus B, 36, 356–366, 1974.

Vali, G.: Nucleation terminology, J. Aerosol Sci., 16, 575–576, doi:10.1016/0021-8502(85)90009-6, 1985.

Vehkamäki, H., Kulmala, M., Napari, I., Lehtinen, K. E. J., Timmreck, C., Noppel, M., and Laaksonen, A.: An improved parameterization for sulfuric acid-water nucleation rates for tropospheric and stratospheric conditions, J. Geophys. Res., 107, 4622, doi:10.1029/2002JD002184, 2002.

Vignati, E., Wilson, J., and Stier, P.: M7: an efficient size-resolved aerosol microphysics module for large-scale aerosol transport models, J. Geophys. Res., 109, D22202, doi:10.1029/2003JD004485, 2004.

Wegener, A.: Thermodynamik der Atmosphäre, J. A. Barth, Leipzig, 1911.

Weingartner, E., Nyeki, S., and Baltensperger, U.: Seasonal and diurnal variation of aerosol size distributions ($10 < D < 750\,\mathrm{nm}$) at a high-alpine site (Jungfraujoch 3580 m asl), J. Geophys. Res., 104, 26809–26820, doi:10.1029/1999JD900170, 1999.

Xue, L., Teller, A., Rasmussen, R., Geresdi, I., and Pan, Z.: Effects of aerosol solubility and regeneration on warm-phase orographic clouds and precipitation simulated by a detailed bin microphysical scheme, J. Atmos. Sci., 67, 3336–3354, doi:10.1175/2010JAS3511.1, 2010.

Xue, L., Teller, A., Rasmussen, R., Geresdi, I., Pan, Z., and Liu, X.: Effects of aerosol solubility and regeneration on mixed-phase orographic clouds and precipitation, J. Atmos. Sci., 69, 1994–2010, doi:10.1175/JAS-D-11-098.1, 2012.

Young, K. C.: A numerical simulation of wintertime, orographic precipitation: Part I. Description of model microphysics and numerical techniques, J. Atmos. Sci., 31, 1735–1748, doi:10.1175/1520-0469(1974)031<1735:ANSOWO>2.0.CO;2, 1974a.

Young, K. C.: The role of contact nucleation in ice phase initiation in clouds, J. Atmos. Sci., 31, 768–776, doi:10.1175/1520-0469(1974)031<0768:TROCNI>2.0.CO;2, 1974b.

Zhao, H.-B. and Zheng, C.-G.: Stochastic algorithm and numerical simulation for drop scavenging of aerosols, Appl. Math. Mech.-Engl., 27, 1321–1332, doi:10.1007/s10483-006-1004-z, 2006.

Zubler, E. M., Folini, D., Lohmann, U., Lüthi, D., Muhlbauer, A., Pousse-Nottelmann, S., Schär, C., and Wild, M.: Implementation and evaluation of aerosol and cloud microphysics in a regional climate model, J. Geophys. Res., 116, D02211, doi:10.1029/2010JD014572, 2011a.

Zubler, E. M., Lohmann, U., Lüthi, D., Schär, C., and Muhlbauer, A.: Statistical analysis of aerosol effects on simulated mixed-phase clouds and precipitation in the Alps, J. Atmos. Sci., 68, 1474–1492, doi:10.1175/2011JAS3632.1, 2011b.

Table 1. Table of the different aerosol modes of the aerosol module M7. (The size range of each mode is given for the count median radius $\overline{r_k}$. N_k and M_k^X correspond to the aerosol number and mass density for the mode $k \in [1,7]$ and compound $X \in \{SU, BC, OC, SS, DU\}$ respectively.) Adapted from Vignati et al. (2004).

Aerosol mode	Size range [μm]	Soluble/internally mixed mode	Insoluble modes
Nucleation	< 0.005	N_1, M_1^{SU}	
Aitken	0.005–0.05	$N_2, M_2^{SU}, M_2^{BC}, M_2^{OC}$	N_5, M_5^{BC}, M_5^{OC}
Accumulation	0.05–0.5	$N_3, M_3^{SU}, M_3^{BC}, M_3^{OC}, M_3^{SS}, M_3^{DU}$	N_6, M_6^{DU}
Coarse	> 0.5	$N_4, M_4^{SU}, M_4^{BC}, M_4^{OC}, M_4^{SS}, M_4^{DU}$	N_7, M_7^{DU}

Table 2. Table of the five in-hydrometeor aerosol modes. M_j^X corresponds to the in-hydrometeor aerosol mass density for the mode $j \in \{CD, RD, IC, SF, GR\}$ and compound $X \in \{SU, BC, OC, SS, DU\}$. (The number mode N_j with $j \in \{CD, RD, IC, SF, GR\}$ is not a prognostic variable, but is diagnosed during evaporation and sublimation from the corresponding hydrometeor number density.)

Aerosol mode	Abbrev.	Mass modes	Number mode
In-cloud droplet mode	CD	$M_{CD}^{SU}, M_{CD}^{BC}, M_{CD}^{OC}, M_{CD}^{SS}, M_{CD}^{DU}$	$N_{CD} = N_c$
In-rain drop mode	RD	$M_{RD}^{SU}, M_{RD}^{BC}, M_{RD}^{OC}, M_{RD}^{SS}, M_{RD}^{DU}$	$N_{RD} = N_r$
In-ice crystal mode	IC	$M_{IC}^{SU}, M_{IC}^{BC}, M_{IC}^{OC}, M_{IC}^{SS}, M_{IC}^{DU}$	$N_{IC} = N_i$
In-snow flake mode	SF	$M_{SF}^{SU}, M_{SF}^{BC}, M_{SF}^{OC}, M_{SF}^{SS}, M_{SF}^{DU}$	$N_{SF} = N_s$
In-graupel mode	GR	$M_{GR}^{SU}, M_{GR}^{BC}, M_{GR}^{OC}, M_{GR}^{SS}, M_{GR}^{DU}$	$N_{GR} = N_g$

Table 3. Parameters of the initial aerosol size distributions (Muhlbauer and Lohmann, 2008) and mass fractional composition (Cozic et al., 2008) with N_a the aerosol number density, r the mode mean radius, σ the standard deviation and M_a the aerosol mass density of the lognormal distribution. Aerosol compounds include organic carbon (OC), black carbon (BC), sulfate (SU) and dust (DU).

Aerosol mode	N_a	r	σ	M_a	Mass fractional composition
Aitken	$530\,\mathrm{cm}^{-3}$	$0.022\,\mu\mathrm{m}$	2.13	$0.27\,\mu\mathrm{g\,m}^{-3}$	66 % OC, 30 % SU, 4 % BC
accumulation	$260\,\mathrm{cm}^{-3}$	$0.070\,\mu\mathrm{m}$	1.61	$1.74\,\mu\mathrm{g\,m}^{-3}$	60 % OC, 28 % SU, 9 % DU, 3 % BC

Table 4. Description of the conducted simulations.

Simulation	Temperature	Aerosol initialization	Description
CTL-w	280 K	all aerosols mixed	standard simulation (Muhlbauer and Lohmann, 2008, 2009)
SCAV-w	280 K	all aerosols mixed	with aerosol activation and below-cloud scavenging (Zubler et al., 2011a)
SCAV-ALL-w	280 K	all aerosols mixed	with activation scavenging, the adapted below-cloud scavenging parameterization and in-cloud collision scavenging
AP-w	280 K	all aerosols mixed	with aerosol processing (including all scavenging processes and aerosol regeneration)
CTL-c	270 K	50 % of DU is insoluble	standard simulation
SCAV-c	270 K	50 % of DU is insoluble	with aerosol activation and below-cloud scavenging
SCAV-ALL-c	270 K	50 % of DU is insoluble	with activation scavenging, the adapted below-cloud scavenging parameterization and in-cloud collision scavenging
AP-c	270 K	50 % of DU is insoluble	with aerosol processing

Table 5. Ratios of the aerosol number concentration of "regenerated" particles (N_{reg}, difference between AP and SCAV-ALL), the total aerosol number concentration in simulation AP (N_{total}), the number concentration of "regenerated" particles potentially acting as CCN (N_{reg}^{CCN}, difference between AP and SCAV-ALL), the number concentration of CCN in simulation AP (N_{total}^{CCN}) and the number concentration of "missing particles due to scavenging" (N_{scav}, difference between SCAV-ALL and CTL) of the sensitivity studies of the warm case. The values are averaged horizontally between 680 and 720 km at 300 m and 2000 m altitude. σ^* denotes the simulations with the M7 standard deviations. The first two lines describe the analyzed warm case.

| $RH_{surface}$	Altitude	Aerosol initialization	N_{reg}/N_{total}	$N_{reg}^{CCN}/N_{total}^{CCN}$	N_{reg}/N_{scav}
90%	300 m	polluted sommer	0.23	0.33	0.24
	2000 m	polluted sommer	0.18	0.32	0.24
85%	300 m	polluted sommer	0.39	0.47	0.36
	2000 m	polluted sommer	0.18	0.35	0.25
80%	300 m	polluted sommer	0.31	0.43	0.26
	2000 m	polluted sommer	0.23	0.39	0.39
90%, σ^*	300 m	polluted sommer	0.23	0.33	0.24
	2000 m	polluted sommer	0.18	0.32	0.24
90%	300 m	clean winter	0.04	0.35	0.12
	2000 m	clean winter	0.08	0.44	0.27
80%	300 m	clean winter	0.05	0.46	0.19
	2000 m	clean winter	0.03	0.38	0.12

Table 6. Ratios of the aerosol number concentration of "regenerated" particles (N_{reg}, difference between AP and SCAV-ALL), the total aerosol number concentration in simulation AP (N_{total}), the number concentration of "regenerated" particles potentially acting as CCN (N_{reg}^{CCN}, difference between AP and SCAV-ALL), the number concentration of CCN in simulation AP (N_{total}^{CCN}) and the number concentration of "missing particles due to scavenging" (N_{scav}, difference between SCAV-ALL and CTL) of the sensitivity studies of the cold case. The values are averaged horizontally between 680 and 720 km at 300 m and 2000 m altitude. σ^* denotes the simulations with the M7 standard deviations. The first two lines describe the analyzed cold case.

$RH_{surface}$	Altitude	Aerosol initialization	N_{reg}/N_{total}	$N_{reg}^{CCN}/N_{total}^{CCN}$	N_{reg}/N_{scav}
90%	300 m	polluted sommer	0.21	0.57	0.04
	2000 m	polluted sommer	0.18	0.38	0.36
85%	300 m	polluted sommer	0.17	0.36	0.04
	2000 m	polluted sommer	0.24	0.48	0.49
80%	300 m	polluted sommer	0.19	0.47	0.07
	2000 m	polluted sommer	0.28	0.49	0.57
90%, σ^*	300 m	polluted sommer	0.21	0.57	0.04
	2000 m	polluted sommer	0.18	0.38	0.36
90%	300 m	clean winter	0.03	0.55	0.03
	2000 m	clean winter	0.02	0.31	0.09
80%	300 m	clean winter	0.01	0.26	0.05
	2000 m	clean winter	0.05	0.43	0.27

41
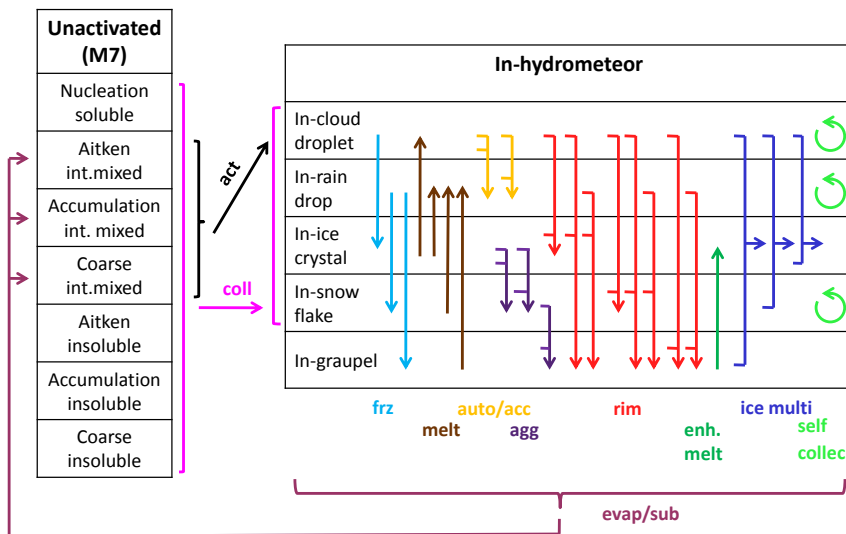
Figure 1. Microphysical transfer processes between the different aerosol modes (coll = in-cloud and below-cloud collision scavenging, act = activation scavenging, frz = freezing, melt = melting, auto = autoconversion, acc = accretion, agg = aggregation, rim = riming, enh. melt = enhanced melting, ice multi = ice multiplication, self collec = self-collection, evap = evaporation, sub = sublimation).
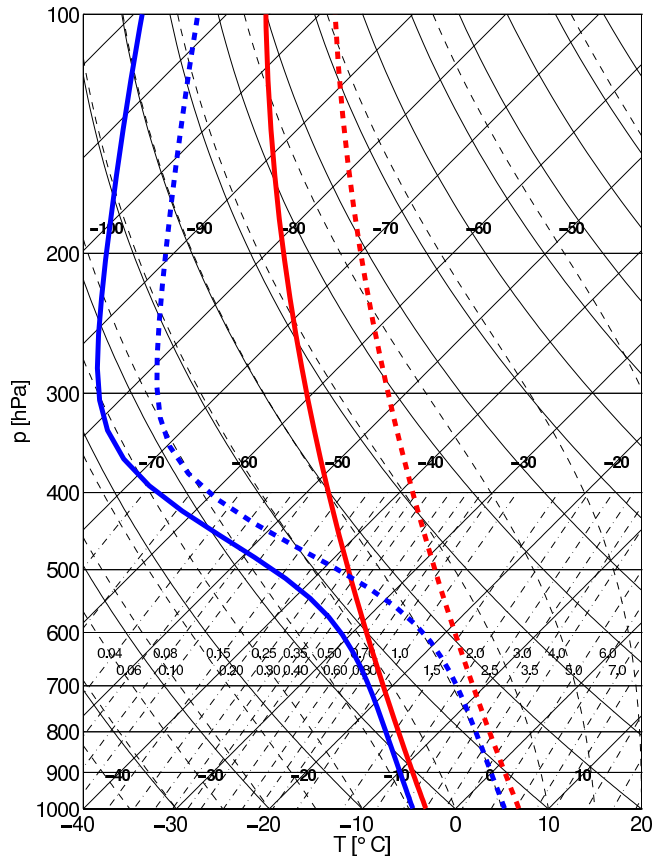
Figure 2. SkewT–logp diagram of the atmospheric soundings for the idealized 2-D simulations showing the temperature (red) and the dew point temperature (blue) with a surface relative humidity of 90 %. The warm sounding (dashed) with a surface temperature of 280 K is used for the simulation of a warm-phase cloud, the cold sounding (solid) with a surface temperature of 270 K is used for the simulation of a mixed-phase cloud.
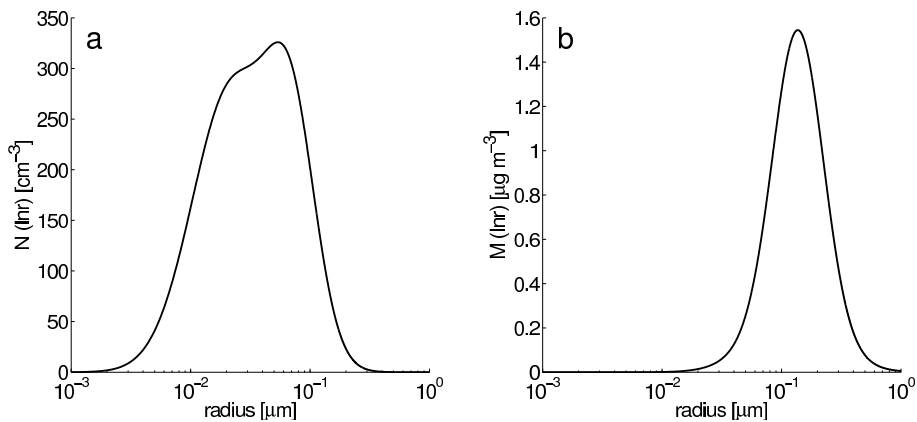
Figure 3. Initial aerosol **(a)** number density and **(b)** mass density size distributions for all simulations.
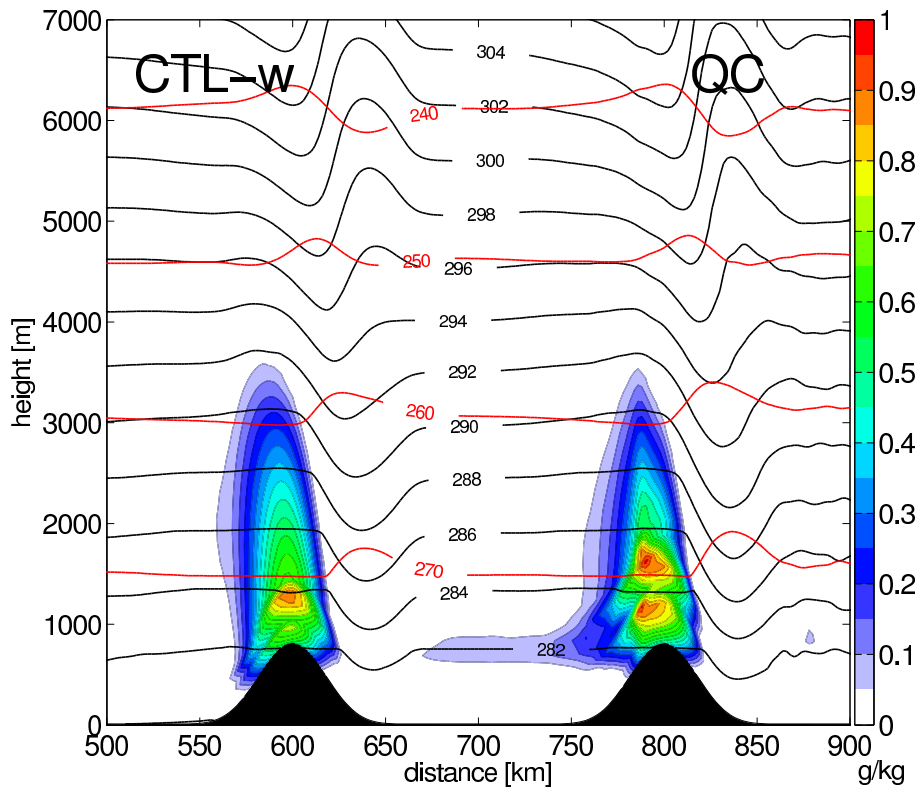
Figure 4. Vertical cross section of the cloud water mixing ratio (QC) for the simulation CTL-w after 10 h. Black lines indicate the potential temperature (K) and red lines the temperature (K). Only part of the computational domain is shown.
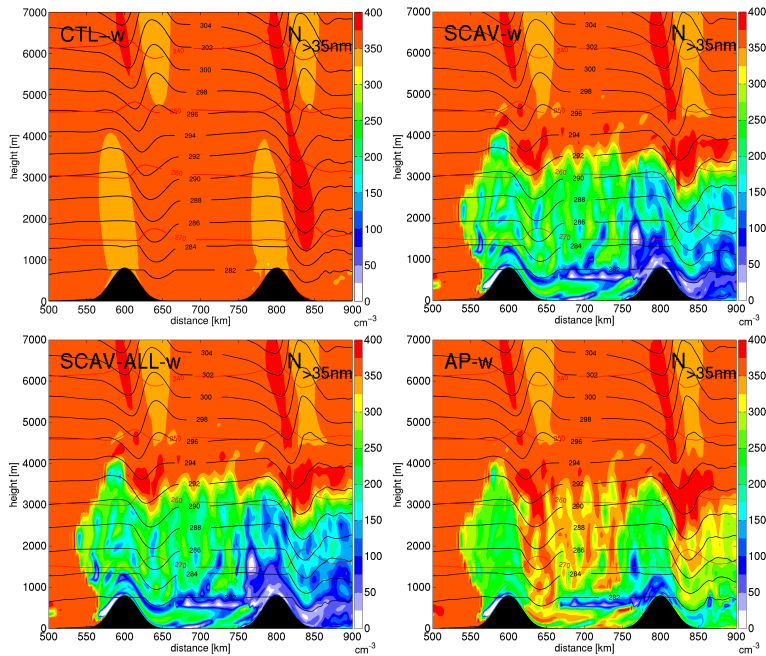
Figure 5. Vertical cross section of the number concentration of aerosol particles larger than $35\,\mathrm{nm}$ ($N_{>35\,\mathrm{nm}}$) which may potentially act as CCN in the model for simulation CTL-w, SCAV-w, SCAV-ALL-w and AP-w after $10\,\mathrm{h}$. Black lines indicate the potential temperature (K) and red lines the temperature (K). Only part of the computational domain is shown.
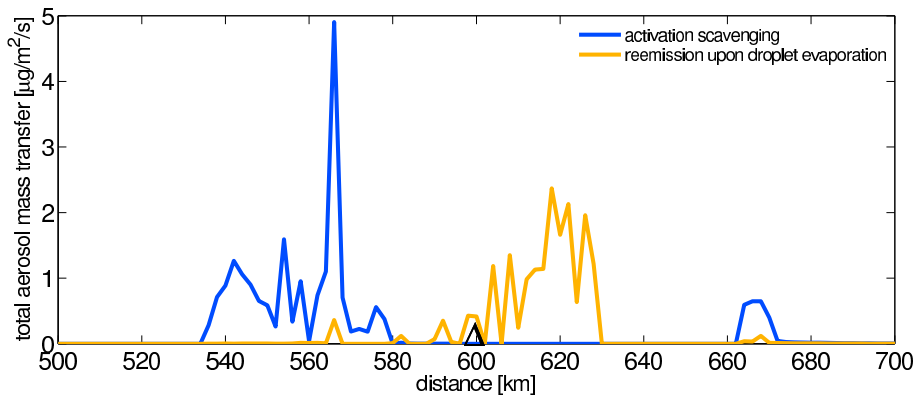
Figure 6. Vertically integrated aerosol mass transfer rates per second of different processes within the microphysical scheme along the flow direction after $10\,\mathrm{h}$ in simulation AP-w over the first mountain (mountain peak represented by the triangle at $600\,\mathrm{km}$). Only aerosol mass transfer rates larger than $0.2\,\mathrm{\mu g\,m^{-2}\,s^{-1}}$ are shown.
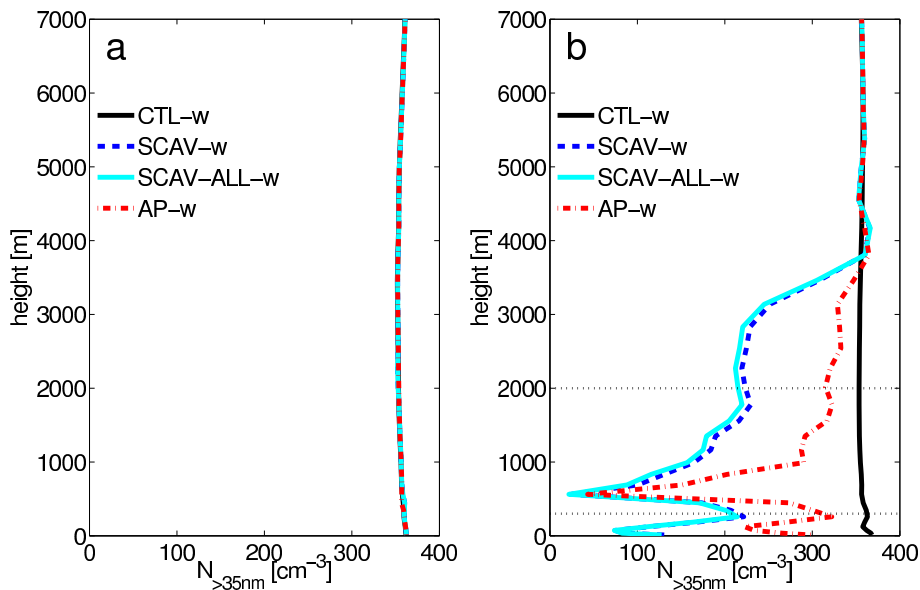
Figure 7. Vertical profile of the number concentration of aerosol particles larger than 35 nm ($N_{>35\,nm}$) after 10 h **(a)** upstream (averaged between 510 and 530 km) and **(b)** downstream (averaged between 680 and 720 km) of the first mountain for the warm cloud cases. Dotted horizontal lines indicate altitudes at which cumulative aerosol size distributions are compiled.
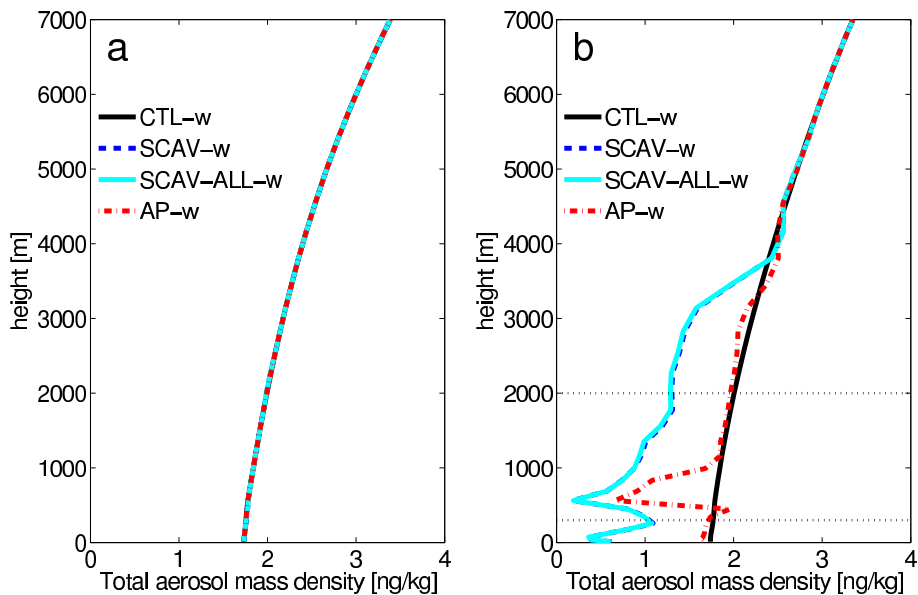
Figure 8. Vertical profile of the total aerosol mass density after 10 h **(a)** upstream (averaged between 510 and 530 km) and **(b)** downstream (averaged between 680 and 720 km) of the first mountain for the warm cloud cases. Dotted horizontal lines indicate altitudes at which cumulative aerosol size distributions are compiled.
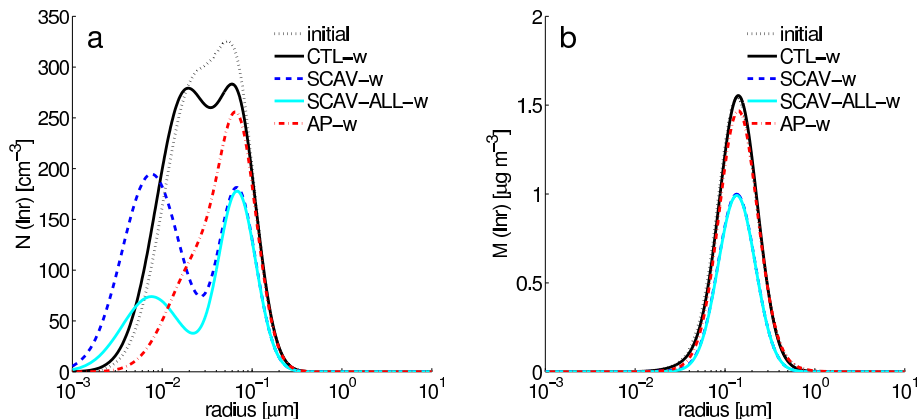
Figure 9. Cumulative aerosol **(a)** number and **(b)** mass size distribution after cloud passage after 10 h for the warm cloud cases. The values are averaged horizontally between 680 and 720 km at 300 m altitude.
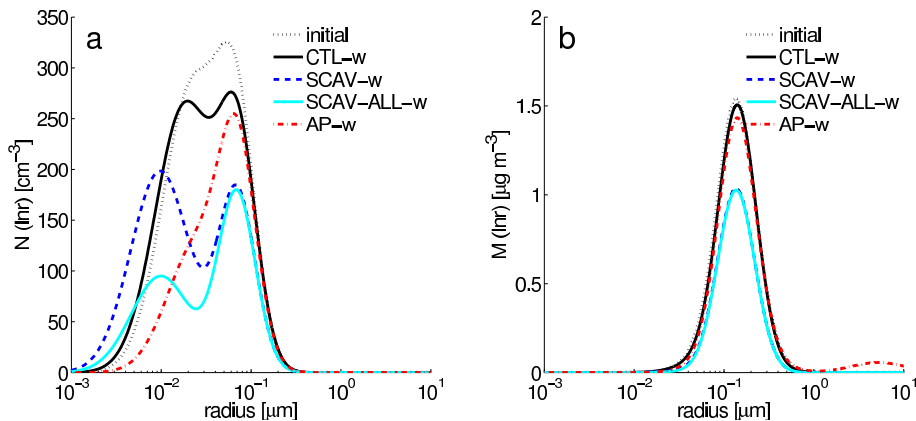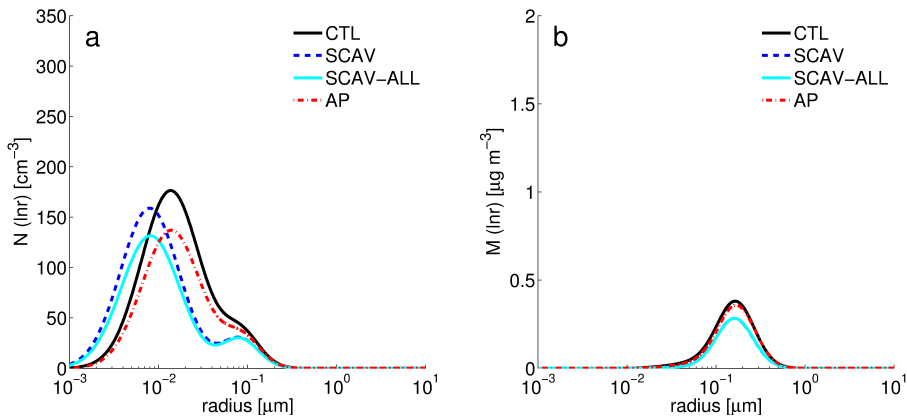
Figure 10. Cumulative aerosol (**a**) number and (**b**) mass size distribution after cloud passage after 10 h for the warm cloud cases. The values are averaged horizontally between 680 and 720 km at 2000 m altitude.
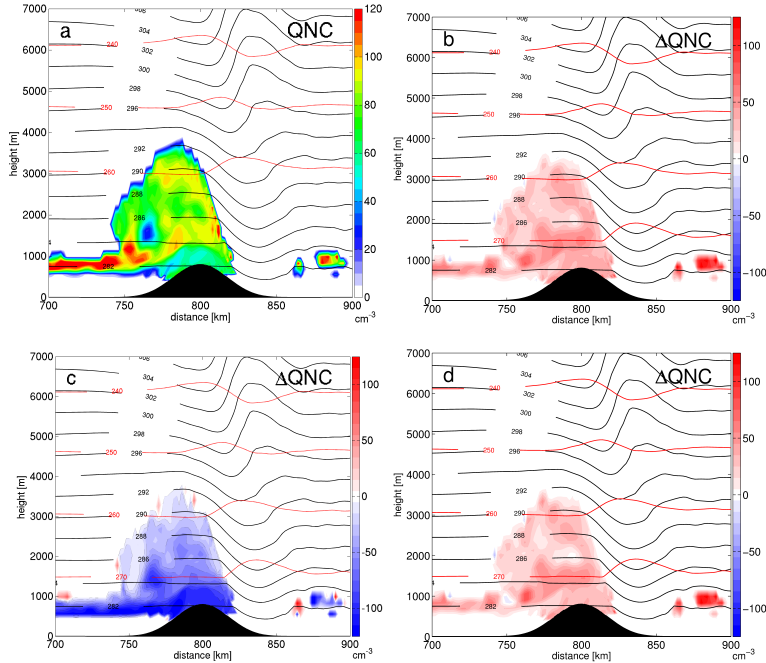
Figure 11. Number concentration of cloud droplets in **(a)** simulation AP-w and difference in cloud droplet number concentration between simulations **(b)** AP-w and SCAV-ALL-w, **(c)** AP-w and CTL-w and **(d)** AP-w and SCAV-w after 10 h over the second mountain. Black lines indicate the potential temperature (K) and red lines the temperature (K). Only part of the computational domain is shown.
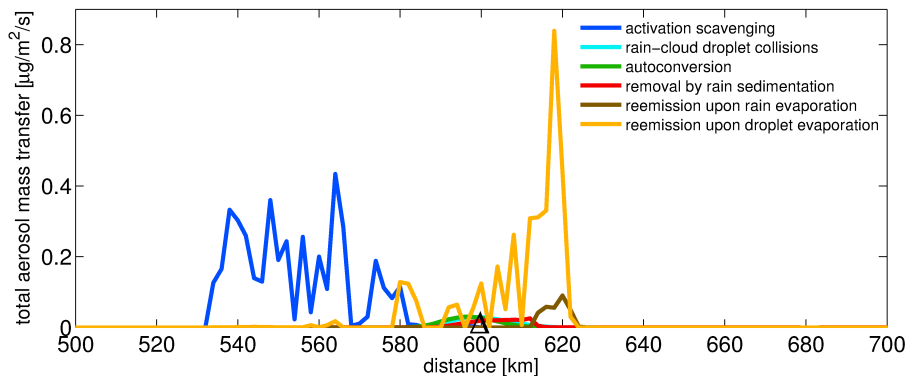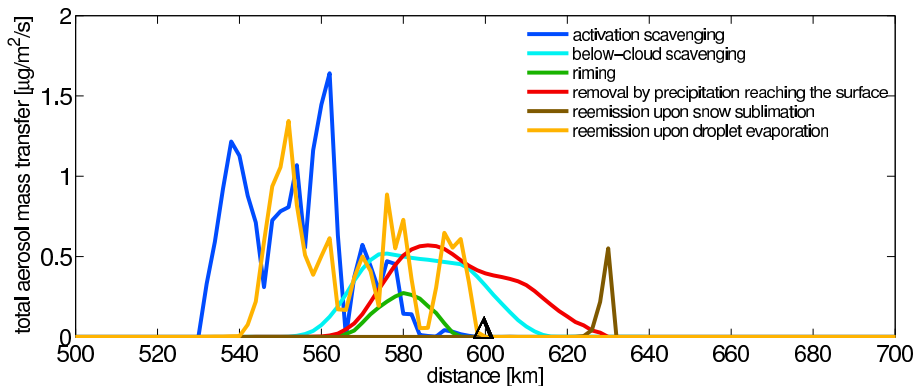
Figure 12. Vertically integrated aerosol mass transfer rates per second of different processes within the microphysical scheme along the flow direction after 10 h in the simulation with aerosol processing for the clean aerosol initialization over the first mountain (mountain peak represented by the triangle at 600 km). Only aerosol mass transfer rates larger than $0.02 \, \mu\mathrm{g}\,\mathrm{m}^{-2}\,\mathrm{s}^{-1}$ are shown.

Figure 13. Cumulative aerosol **(a)** number and **(b)** mass size distribution after cloud passage after 10 h for the warm simulations with clean aerosol initialization. The values are averaged horizontally between 680 and 720 km at 300 m altitude.
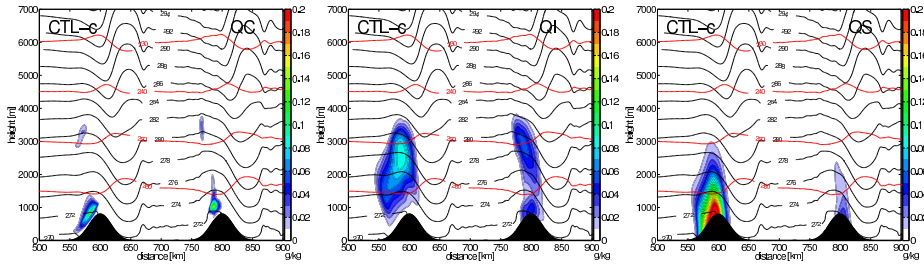
Figure 14. Vertical cross section of the cloud water mixing ratio (QC), ice water mixing ratio (QI) and snow water mixing ratio (QS) in simulation CTL-c after 10 h. Black lines indicate the potential temperature (K) and red lines the temperature (K). Only part of the computational domain is shown.

Figure 15. Vertically integrated aerosol mass transfer rates of different processes within the microphysical scheme along the flow direction after $10\,\mathrm{h}$ in simulation AP-c over the first mountain (mountain peak represented by the triangle at $600\,\mathrm{km}$). Only part is of computational domain is shown. Only aerosol mass transfer rates larger than $0.2\,\mu\mathrm{g}\,\mathrm{m}^{-2}\,\mathrm{s}^{-1}$ are shown.
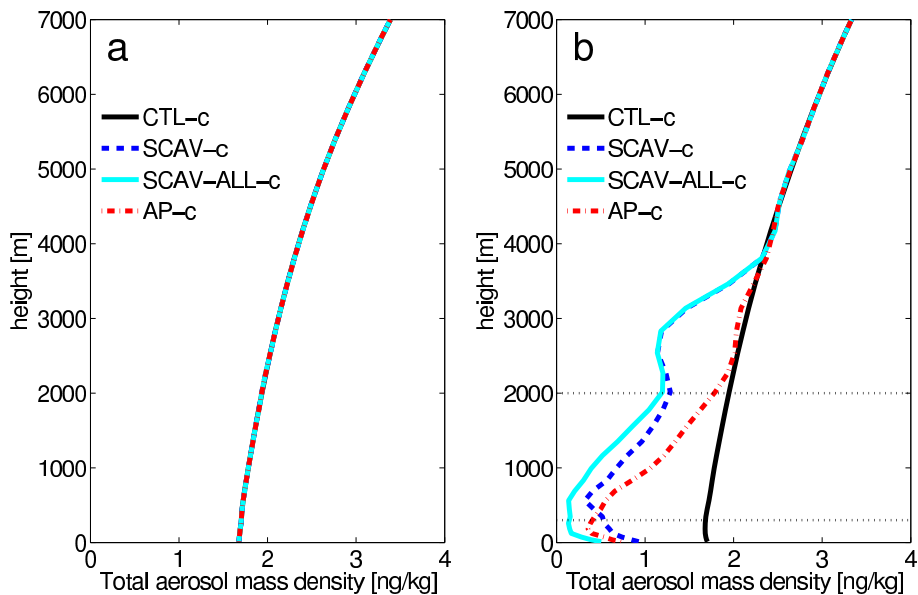
Figure 16. Vertical profile of the total aerosol mass density after 10 h **(a)** upstream (averaged between 510 and 530 km) and **(b)** downstream (averaged between 680 and 720 km) of the first mountain for the cold cloud cases. Dotted horizontal lines indicate altitudes at which cumulative aerosol size distributions are compiled.
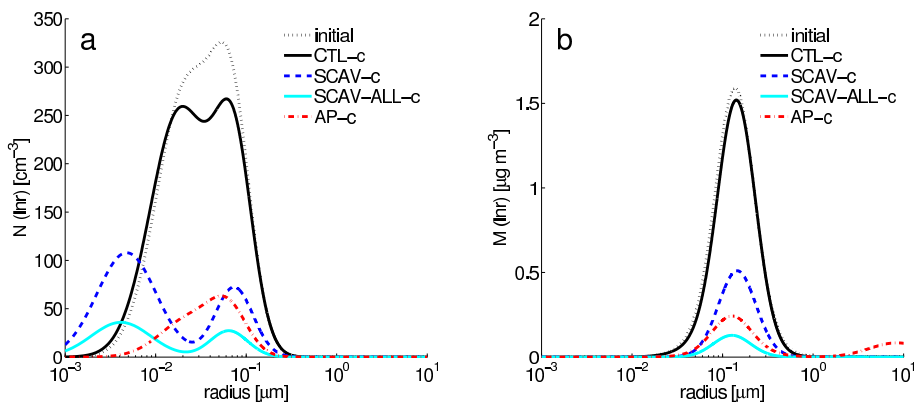
Figure 17. Cumulative aerosol **(a)** number and **(b)** mass size distribution after cloud passage after 10 h for the cold cloud cases. The values are averaged horizontally between 680 and 720 km at 300 m altitude.
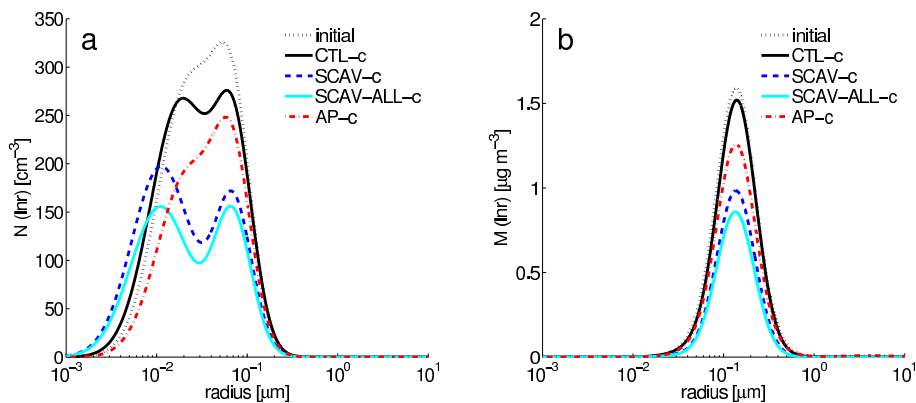
Figure 18. Cumulative aerosol **(a)** number and **(b)** mass size distribution after cloud passage after 10 h for the cold cloud cases. The values are averaged horizontally between 680 and 720 km at 2000 m altitude.
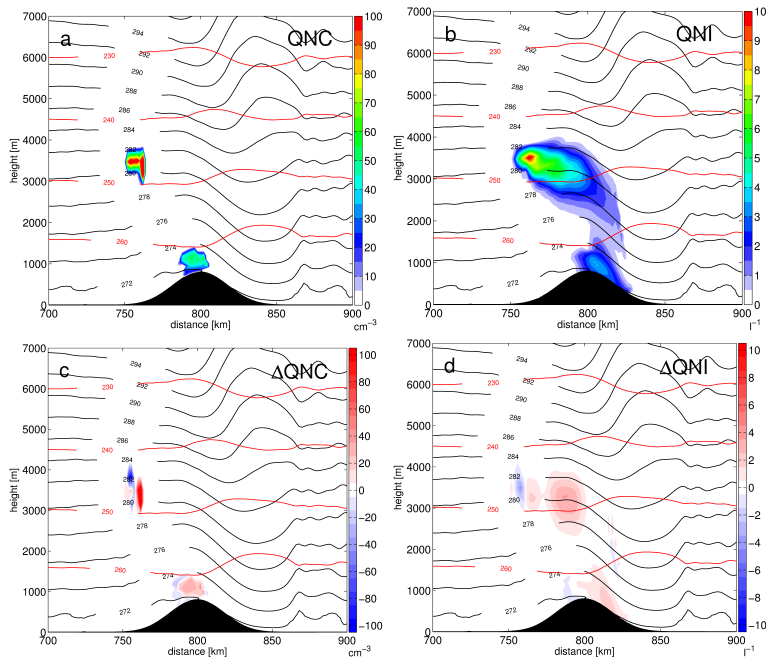
Figure 19. Number concentration of **(a)** cloud droplets and **(b)** ice crystals in simulation AP-c and difference between simulation AP-c and SCAV-ALL-c in **(c)** cloud droplet number concentration and **(d)** ice crystal number concentration after 10 h over the second mountain. Black lines indicate the potential temperature (K) and red lines the temperature (K). Only part of the computational domain is shown.